energies

MDPI

Article

A Graph-Theoretic Approach for Optimal Phasor Measurement Units Placement Using Binary Firefly Algorithm

Onkemetse Tshenyego [1,*], Ravi Samikannu [1], Bokani Mtengi [1], Modisa Mosalaosi [1] and Tshiamo Sigwele [2]

[1] Department of Electrical, Computer and Telecommunications Engineering, Botswana International University of Science and Technology, Palapye, Botswana; ravis@biust.ac.bw (R.S.)
[2] Department of Computer Science and Information Systems, Botswana International University of Science and Technology, Palapye, Botswana
* Correspondence: tshenyegoo@biust.ac.bw

Abstract: The pursuit of achieving total power network observability in smart grids using Phasor Measurement Units (PMUs) carries a significant promise of real-time Wide-Area Monitoring, Protection, and Control (WAMPAC). PMU applications eliminate periodical measurements, thereby increasing accuracy through a high sampling rate of the measured power systems quantities. The high costs of installation of PMUs for total power system observability presents a challenge in the implementation of PMUs. This is due to the expensive costs of PMU devices. This has led to a prominent optimal PMU placement (OPP) problem that researchers tirelessly aim to solve by ensuring a complete power network observability while using the least installed PMU devices possible. In this paper, a novel Binary Firefly Algorithm (BFA) based on the node degree centrality scores of each bus is proposed to minimize PMU installations. The BFA solves the OPP problem in consideration of the effect of Zero Injection Buses (ZIBs) under normal operation and single PMU outage (SPO). The robustness and efficiency of the proposed algorithm is tested on IEEE-approved test systems and visualized with a force-directed technique on an undirected power network graph. The proposed BFA yields the same but better optimal PMU numbers, obtained by existing meta-heuristic optimization techniques found in the literature for each of the IEEE test cases, as well as highlighting the cost–benefit of having a robust system against single PMU loss while considering the ZIB effect for an improved system measurement availability.

Keywords: binary firefly algorithm; node degree centrality; optimal PMU placement; single PMU outage

Citation: Tshenyego, O.; Samikannu, R.; Mtengi, B.; Mosalaosi, M.; Sigwele, T. A Graph-Theoretic Approach for Optimal Phasor Measurement Units Placement Using Binary Firefly Algorithm. *Energies* **2023**, *16*, 6550. https://doi.org/10.3390/en16186550

Academic Editors: Rene Prenc, Dubravko Franković and Vitomir Komen

Received: 28 June 2023
Revised: 28 July 2023
Accepted: 3 August 2023
Published: 12 September 2023

1. Introduction

In the hierarchically distributed architecture of the WAMPAC system proposed in [1], in the data acquisition layer lies the Phasor Measurement Unit (PMU). PMU devices collect the magnitude, frequency, phase, and rate of change of the frequency of sampled AC voltage and current, measured using voltage and current transformers from different geographical locations of the smart grid [2]. PMUs perform this accurately in real-time with remarkable reporting rates in the order of tenths of Hz [3]. To be more specific on the reporting rates, two classes of PMUs are considered, the Monitoring class (M class) and the Protection class (P class). These classes of PMUs conform to the 2014 amendments of the IEEE C37.118.1-2011 [4] that dictates data rate specifications of 25 and 50 frames/second on a system running at 50 Hz, while a system running at 60 Hz must be configured for 30 and 60 frames/second for M class. P class, on the hand, requires a higher resolution for an advanced and accurate system parameter tracking and has data rate specifications of 10, 25 and 50 frames/second on a 50 Hz system and 10, 12, 15, 20, 30 and 60 frames/second for systems running at 60 Hz. PMU brands that are currently available in the market, such as the MiCom Agile P847, carry out the transmission of Coordinated Universal Time (UTC)-synchronized measurement information, termed the synchro-phasor, based on

IEEE C37.118, using TCP/IP and UDP/multicast. Current transformer (CT) and voltage transformer (VT) inputs available on a single PMU are also important constraints to consider when solving the OPP problem because, the higher the number of channels, the higher the number of lines that can be measured. MiCom Agile P847 is available in 3 CT/3 VT, 6 CT/6 VT or 12 CT/6 VT measurement channel inputs [5]. The synchro-phasor data are transmitted to the Phasor Data Concentrator (PDC) where real-time monitoring, protection, and post-event analysis of the electric power network are performed [6]. This information is synchronized using the Coordinated Universal Time (UTC) as a common time source. The measurement synchronism is crucial for state estimation, as a time-stamped snapshot of the entire grid in terms of measurements is attainable and can be compared with the previous one stored in the historian. To date, the merits of PMU application to solve the ever-growing challenges of the grid remains undefeatable, but the PMU cost is a major limiting factor when considering the quantity of PMU devices that can be installed for a complete power network observability [7]. A single PMU costs between USD 40,000 and USD 180,000 for procurement, installation, and commissioning [8]. A PMU is not a standalone device; its hardware cost only amounts to 5% of the synchro-phasor systems' installation costs. This shows that the total system costs are higher and any opportunity to reduce installation costs must be considered. Upon the realization of the fact that it is not necessary to install a PMU on every bus to achieve a full observability of the grid [9], researchers are in pursuit to exploit this window of opportunity to find the optimal PMU placement with a great reduction in PMU installation costs. By achieving this, there will be a seamless transition from traditional power grids to smart grid technologies, leading to real-time protection and monitoring under a complete power system observability.

State-of-the-Art OPP Algorithms

Ever since the introduction of PMUs in the 1980s to power systems for monitoring and protection purposes, significant research strides aiming at PMU installation cost reduction using variable research methods and approaches to the subject matter have been observed. The taxonomy of techniques used in solving the OPP problem is well-articulated in [10,11], and the most updated review of these methods is presented in Table 1. Optimum PMU placement stems from the classical problem formulation, which the authors of [12–14] have explored to find a cost-effective device installation with while adhering to complete grid observability. A variety of meta-heuristic methods with the ability to solve discrete parameters and non-continuous cost functions have been captured in [15]. In [16], an immunity genetic algorithm using bio-objectives to find the number of PMUs while considering measurement redundancy minimization is proposed. The authors of [17] used a genetic algorithm to find Pareto optimal solutions in a graph-theoretic setup using Nondominated Sorting Genetic Algorithm (NSGA). The attractive feature of this approach was based on NSGA's ability to find the best optimal Pareto solution as opposed to simply one solution, a feature that makes it applicable for multi-objective optimization problems in large search spaces. Recently, the authors of [18] applied the NSGA-II algorithm to distribution systems solving for the total number of PMU channels and maximum state estimation uncertainty on high-rate device measurements, and similarly in [17], their study showed a convergence to a Pareto frontier of solutions. In [19], numerical observability using Branch-and-Bound (BB), alongside a Binary Coded Genetic Algorithm (BGCA), in consideration of conventional measurements and ZIBs is investigated. In this approach, the BB algorithm pinpoints the global minimum, while BCGA locates non-peculiar global optimum solutions. A greedy-based PMU placement algorithm is proposed alongside Convolutional Neural Networks (CNNs) in [20]. In this approach, a data-driven PMU placement algorithm optimizes the loss function of the CNN to perform fault localization. A similar work to [20] that considers faulted line detection is proposed in [21], in which a bi-level optimization problem that takes into account the PMU channel limitation is presented and used to solve the OPP. In this approach, an upper level uses Particle Swarm Optimization (PSO) to find a global solution with the consideration of the effect of unutilised PMU channels from a PMUs deployable. The

second level of this approach uses Integer Linear Programming (ILP) to find the placement from which line observability is obtained. In [22], a novel scalable solver for significantly large binary optimization problems with unknown solutions is developed. This is achieved through modelling function approximations that can perform scalable computations with binary optimization penalty. Stochastic-based population optimization techniques were used in [6,23]. In [24], Exponential Particle Swarm Optimization (EBPSO) algorithm is proposed; results from the EBPSO algorithm proved that nonlinear inertia weight coefficient improves the searching ability through modifications of the particle position-updating equations. Integer quadratic programming, mixed integer programming, and equivalent integer linear programming are some of the mathematical methods that have been used to solve the OPP [25]. A more recent article [26] considers PMU placement in the light of small-signal stability assessment (SSSA). This is achieved by using SSSA alongside system observability probability, PMU cost, and transmission lines in a multi-objective SSSA-OPP. All the methods mentioned in this section thus far were used to solve the OPP with regard to topology issues and contingencies separately. Recently, a new paradigm shift is observed as researchers merge bus topology arrangements with other contingencies in their quest to reduce PMU installations while maximizing measurement redundancy for a complete EPS observability. In these new directions, the authors of [27] used the Crow search algorithm to solve the OPP for a single PMU outage (SPO) with the ZIB effect, single line loss with the ZIB effect, and PMU channel limits with the ZIB effect. According to their research efforts, topological observability with a consideration of the ZIB effect and channel limit with ZIB effect yields the lowest optimal number of PMUs; but is the system secure to operate under these conditions? The security benefits of measurement channel limitations are superseded by those of single line loss, especially for the observability of buses with no PMUs installed. However, it is even more catastrophic to lose a PMU in the data acquisition layer of the WAMPAC system as it affects both topological observability under normal considerations and any contingency. This exposes the current gap in the OPP problem that can be filled by ensuring that the lowest optimal PMU number is achieved by an algorithm that satisfies SPO constraint, while keeping PMU numbers low by using the ZIB effect.

Table 1. A literature review of existing OPP techniques.

Refs.	Year	Contributions	Techniques	Test Systems	Topology and Sensor Issues	Observability Metrics	Contingencies Considered	Achievements
[27]	2022	New meta-heuristic approach in solving the OPP presenting multiple solution sets. Solves contingencies with and without ZIB consideration.	Crow Search Algorithm (CSA)	14-bus, 30-bus, 57-bus, 72-bus	Effect of ZIB, and channel limits	Total System Observability Redundancy Index (TSORI)	N-1 PMU loss, N-1 line loss with and without ZIB effect	CSA solves the OPP for multiple PMU placement sets for the same optimal PMU number, allowing for better redundancy set to be selected.
[28]	2020	Modifications of observability propagation rules. Formulated the OPP problem with bounded OPDs.	Mathematical programming	39-bus, 57-bus, 118-bus	Effect of ZIB, conventional measurements, and channel limits	Observability Propagation Depth (OPD)	N-1 PMU loss, N-1 line loss, and N-1 PMU or N-1 line loss	Exposes the risk of unlimited observability propagations under different contingencies.
[29]	2020	Novel formulations of various topological and contingencies.	Mathematical formulations based on topology and system disturbances effects	68-bus, and 140-bus	Effect of parallel lines, effect of ZIB, PMU channel limits, and pre-existing measurements	None	N-1 line loss	The proposed methodology demonstrates the ability to find fewer optimal PMUs under the largest single line outages possible.

Table 1. *Cont.*

Refs.	Year	Contributions	Techniques	Test Systems	Topology and Sensor Issues	Observability Metrics	Contingencies Considered	Achievements
[30]	2020	Modelling of linear observability constraints using channel limits, ZIB effect, and existing measurements.	Integer Linear Programming (ILP)	14-bus, 30-bus, New England 39-bus, 57-bus, and 118-bus	Effect of ZIB, and channel limitations	None	N-1 and N-2 PMU loss	Introduction of linear and compact forms of observability constraints.
[31]	2019	Novel use of a meta-heuristic algorithm with modifications of classic OPP formulation.	Constriction Factor Particle Swarm Optimization (CF-PSO) and Mixed Integer Linear Programming (MILP)	14-bus, 30-bus, New England 39-bus, 118-bus, Polish 2383-bus, Polish 2736-bus, and Polish-3120-bus	Channel limitations under various contingencies	TSORI and Bus Observability Index (BOI)	N-1 and N-2 PMU loss	Demonstrates the power of meta-heuristic methods in finding more than one solution for the same number of optimal PMU, thereby increasing the chances of finding high measurement redundancy.
[32]	2019	Solves MINLP framework using a two-phase Branch-and-Bound algorithm (BBA), starting with PMUs pre-assigned to each bus to a radial bus.	Mixed Integer Nonlinear Programming (MINLP) formulation solved by Branch-and-Bound Algorithm (BBA)	14-bus, 30-bus, New England 39-bus, 118-bus, and 246-bus	Effect of ZIB, and channel limitations	None	N-1 PMU loss and N-1 line loss	Radial buses are excluded from optimal design as two-phased Branch-and-Bound finds several optimum points.
[33]	2018	OPP model that considers ZIB, proposed a new ZIB-based metric.	Integer Linear Programming (ILP)	14-bus, 30-bus, 39-bus, 118-bus, 300-bus, Polish 2383-bus, Polish	Channel limitations	Zero Injection Utilization Rate (ZIUR) Zero Injection Observability Depth (ZIOD)	N-1 PMU loss, and N-1 line loss	The proposed ZIOD metric is a reliable measure of system reliability.

The contributions of this paper are as follows:

1. This paper proposes a Binary Firefly Algorithm (BFA) for optimal PMU placement in a degree centrality-ranked undirected graph search space. In this approach, the algorithm demonstrates the ability to locate the global minima through a descending node degree centrality score search manner.
2. This paper investigates the possibility of finding a balance in PMU installation costs and observability reliability by a consideration of topological network issues coupled with practical contingencies using established observability performance metrics.

This paper is structured into six sections. Power system observability analysis is covered in Section 2, and the proposed methodology is articulated in Section 3. In Section 4, tests and simulation study procedures are explained to pave the way for illustrative results and the results discussion is carried out in Section 5, followed by the conclusion in Section 6.

2. Power System Observability Analysis

This section reviews the classical formulation types of observability methods in power systems. The fundamental goal in solving the OPP problem is to ensure that the power system network is completely observable. This process is dependent on the state estimation of the entire grid network from the synchro-phasor data collected from PMUs installed

at various selected points in the power system network. Fundamentally, there are two analysis techniques that may be used for observability analysis: topological observability analysis and numerical or algebraic analysis.

The concept of observability stems from the modern control theory, from which any system is deemed observable at state $x(t_0)$ at time t_0 if and only if that state can be determined from the output(s) in finite time. Once system observability is attained, state estimation becomes possible. The relationship between the state and the measurement is described by the following measurement model in accordance with the authors of [34]:

$$\overline{z} = h(\overline{x}) + \overline{e} \tag{1}$$

where (when applied to power systems) $\overline{z}$ is the measurement vector, $h(x)$ is a nonlinear function associated with the state vector and measurement vector, $\overline{x}$ is the state vector of the system containing the voltage phasor for all buses, and $\overline{e}$ is the vector that carries the noise and measurement error information. PMUs are very accurate, making the $\overline{e}$ negligible and leading to a linear estimate of the description $\overline{z} = \mathbf{H}\overline{x}$, where, for n bus system requiring m PMUs, the dimension of the vector $\overline{x}$ is $2n - 1$. Also, the Jacobian matrix **H,** constructed from H_i submatrices obtained from substations where PMUs are installed, has dimensions $m \times (2n - 1)$. The observability of the system is satisfied when the Jacobian matrix is of full rank, i.e., Rank$(\mathbf{H}) = 2n - 1$.

Topological observability, on the other hand, is a more practical approach in which every bus in the power system network becomes observable by at least one PMU. It follows that to solve the OPP problem in any given n-bus system under topological observability, the aim is to minimize the number of PMUs installed while ensuring that every bus in the grid remains observable, as indicated in [6,12]. The objective function is such that

$$min \sum_{i=1}^{N} c_i y_i \tag{2}$$

$$\text{subject to } \mathrm{F}(\overline{Y}) \geq \overline{b}$$

where c_i is the PMU installation cost at an optimal location found at bus i, the vector $\overline{b}$ is such that $\overline{b} = [1, 1, 1, \ldots, 1]^T_{1 \times N}$ if the aim is to make the system fully observable, and y_i is the PMU binary decision entry, such that

$$y_i = \begin{cases} 1 & \text{if a PMU is installed on bus i} \\ 0 & \text{otherwise} \end{cases} \tag{3}$$

These binary entry decisions make up a vector $\overline{Y} = [y_1, y_2, y_3, \ldots, y_N]^T$. The observability constraint vector function is as follows:

$$F(\overline{Y}) = \overline{Y} \times \boldsymbol{A} \quad \geq 1 \tag{4}$$

where $\boldsymbol{A}$ is a symmetric adjacency matrix with a_{ij} constructed from an n-bus system. The connection of elements a_{ij} in $\boldsymbol{A}$ is such that

$$a_{ij} = \begin{cases} 1 & \text{if } i = j \\ 1 & \text{if Bus } i \text{ and Bus } j \text{ are connected} \\ 0 & \text{otherwise} \end{cases} \tag{5}$$

2.1. Topological Observability Case Factors

The observability of the EPS is defined as the process of performing a state estimation of the entire EPS based on a set of availed measurements. These measurements can be obtained from PMUs deployed in a widely distributed power network spanning a vast

geographical area. Measurements that make observability analysis possible are local substation, direct, pseudo, and virtual measurements as considered in this paper. In consideration of the PMU placement model used, a bus refers to a real-life substation where a PMU measures all branches connected to it, including its bus bar. Once the measurements are collected, two types of observability analyses can be used to solve the power system state estimation, these are numerical observability, in which the solution depends on whether the Jacobian matrix is of full rank, and topological observability analysis, in which information of network connectivity, bus type, location, and measurement types are inputs to constructing a network graph used as a search space by OPP algorithms.

2.1.1. Normal Operation without ZIB Effect

In an electric power system, a bus is deemed observable if a PMU installed on a particular bus can measure voltage and brunch current from it using different times of measurements covered in the previous section. Observability through pseudo measurements involves using Kirchhoff's Current Law (KCL) and Ohm's law to calculate the voltages and branch currents of all neighbouring buses to a PMU-installed bus. The following are PMU placement rules:

1. A PMU installed at a given bus measures the voltage and current phasors of all incident branches; therefore, all incident branches are directly observable.
2. Voltage and current phasors at one end of the branch can be calculated using Ohm's law if the voltage at the other end of a branch current is known, resulting in all neighbouring buses being observable.
3. If the voltage phasors of two connected buses are known, KCL is used to calculate the branch current phasor.

2.1.2. Normal Operation with ZIB Effect

In power systems, a bus with a sum of branch currents adding up to zero when KCL is applied to it and has no generator is referred to as a Zero Injection Bus (ZIB). The absence of a generator and current injection makes ZIBs important buses for consideration when solving the OPP as their presence can result in an unobservable bus becoming observable. Therefore, for the grid network, the number of ZIBs in the system represents several buses that do not need to have their power measurements directly taken from. Consequently, this reduces the number of PMU installations required to achieve total network observability. When considering the effect of ZIBs in any power system network, the proposed algorithm PMU placement is guided by the following rules:

1. If there exists an observable ZIB with all adjacent buses being observable except only one of them, the unobservable bus, through the ZIB effect, becomes observable, as Kirchhoff's current law can be used to calculate the unknown voltage phasor to the ZIB.
2. For an unobservable ZIB that has neighbours with known voltage phasors, then the ZIB is deemed to be observable as its voltage phasors can be calculated using its node equation.
3. For the unobservable ZIB group with voltage phasors of its neighbouring buses being known, the nodal equation can be used to calculate the voltage phasors of every unobservable ZIB, making them observable.

2.2. Practical Constraints Case Factors

Single PMU Outage

The security of a power network is of the highest concern in this of era high electrical power reliance. A malfunction of equipment along the transmission and distribution of power may lead to catastrophic consequences like large-scaled blackouts and halted sensitive operations across many sectors, especially in the health sector. Single line loss compromises the observability of buses that PMUs are not placed at; furthermore, pseudo measurements collected through those buses will be lost, becoming a ripple of unobservability of buses with respect to the lost line. If PMU drops out of service due to a malfunction,

all transmission lines and some buses linked to it may become unobservable. This may increase chances of failure of online power-system monitoring and protection strategies, as a portion of the grid is unobservable. The public, wildlife, personnel, power system equipment, and the environment may be at risk of electrocution, cascading faults, and veld fires. To improve the reliability of power transmission, distribution, and delivery to customers, it is worthwhile to consider this problem in the efforts to find optimal PMU placement solutions. To mitigate this constraint, every bus bar must be observed at least by two PMUs. This particular contingency is found to be investigated only under direct and pseudo measurements in most of the source consulted except in [27]. In this paper, a SPO is considered with the effect of ZIB measurements to reduce the PMUs installed even further while achieving a Bus Observability Index (BOI) score of 2 for every bus in the placement set under any kind of measurement.

3. Proposed Method

3.1. Graph Topological Observability

An adjacency matrix is used to construct an undirected network graph $G = (V, E)$, where V and E are the finite sets of vertices or nodes and edges, respectively [35]. For a power system network, a full spanning tree of N vertices represents buses, while edges represent brunches. This network graph becomes the search space that the meta-heuristic methods' search agents transverse to solve the OPP. In finding the optimal PMU placement set, the aim is to find a subgraph $G' = (V', E')$ such that the constraint function in (4) is satisfied, i.e., voltage and branch currents' information from all buses are accessible [36,37].

3.2. Search Space Visualization

In the implementation of the proposed algorithm in MATLAB, once the IEEE dataset is received, an adjacency matrix is extracted from the dataset, detailing the connection between buses. This adjacency matrix is used to construct an undirected graph in which a connection between *bus i* and *bus j* is indicated by bit 1, and bit 1 in the main diagonal signifies a self-loop or, where there is no connection, is otherwise represented by bit 0. This approach of using the adjacency matrix is not effective for large datasets as search agents are forced to transverse the entire search space even points with bit 0. The computational burden increases as the search space becomes larger and larger, and the memory required to handle such computations may not be available. Thus, to combat this problem, a sparse matrix that only stores the nonzero elements of $\boldsymbol{A}$ is constructed. The sparse matrix is a two-dimensional matrix that preserves the node-to-node connection information but with the comparative advantage of a reduced foot-print on the computer's memory. This enables the search agent to only transverse nonzero points of the search space to find the optimal PMU placement set. The proposed meta-heuristic algorithm aims to find a node index that, when bit 0 in the placement vector $\overline{Y}$ is replaced with bit 1, will make as many unobservable nodes as observable as possible, hence the use of Equations (6) and (8). Nodes with such an impact have a high degree centrality score C_D, which is merely a form of node importance in terms of connectivity in the network. This automatically ensures that radial busses are evaded as they have lower C_D scores than most. The number of edges/branches incident to bus i is referred to as the node degree d_i, given by (6):

$$d_i = \sum_{j=1}^{N} a_{ij} - 1 \tag{6}$$

which is used to compute degree centrality $C_D(i)$ given by (7):

$$C_D(i) = d_i/n - 1 \tag{7}$$

Once all the degree centrality scores of every node from the given undirected power network graph are obtained, node ranking can be performed as shown in Figure 1 in which

the numbers in the figure area node IDs and nodes are shaded from blue (lowest C_D score) to violet (highest C_D).

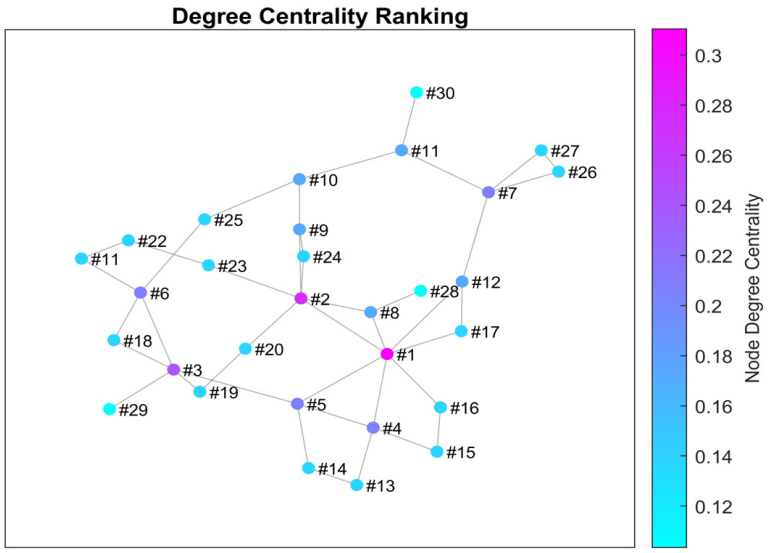

Figure 1. Bus system degree centrality scores.

3.3. Radial Buses Avoidance

In a power system network graph, radial nodes have a degree of one. In consideration of PMU cost reduction, it is not economical to install PMUs on radial buses. According to the authors of [38], it is justified to avoid radial buses as candidates that make up a system PMU placement set as it will only use two channels to monitor the radial bus and its neighbour. In this paper, a strategy to avoid PMU placement solemnly relies in utilizing node degree centrality scores as employed in the BFA algorithm.

3.4. Topological Network Transformation with Consideration of ZIBs

The proposed algorithm considers the ZIB locations in the network before the search agent's action. This process involves inspecting the location of each ZIB and its neighbours in a degree centrality-ranked network and merging that ZIB with a neighbour with the highest degree centrality score. By merging ZIBs with a neighbouring bus with the highest degree centrality score ensures consistency in PMU reduction processes as high-degree-centrality-scoring buses are the best PMU placement nodes for a search agent traversing the search space in a descending node score manner. This also reduces the search space significantly and results in fewer search paths. In this merging process, if there existed a link between a ZIB and another bus other than the one it is being merged with, the links are preserved. This means that if, before the transformation, any bus **X** that was connected to the ZIB—which was merged with bus **T**, forming **T***—and a PMU are placed at a **T**, then bus **X** is deemed observable through the ZIB effect by a PMU placed at bus **T**. This process is illustrated in Figures 2 and 3 below. In Figure 2, node 7 is the ZIB shaded in red and node 4 is its most connected neighbour; therefore, nodes 7 and 4 are merged. If during the search agent trajectory, node 4 fulfils the PMU placement criterion, as shown in Figure 3, and a PMU is placed (shaded green), then node 8, which is shaded orange, becomes observable through the ZIB effect.

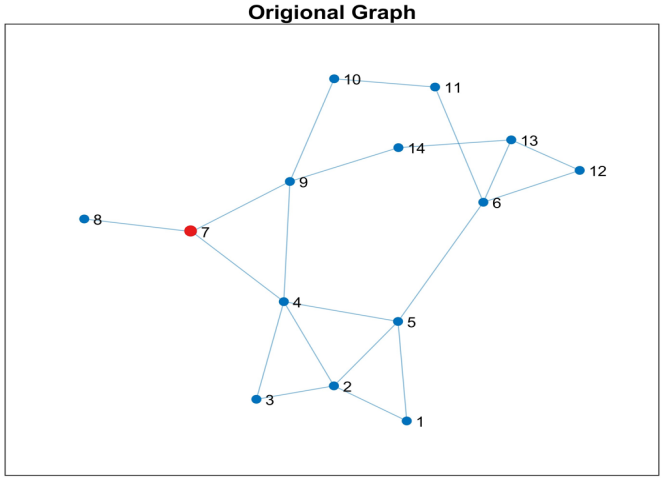

Figure 2. Original IEEE 14-bus undirected graph with ZIB highlighted (red).

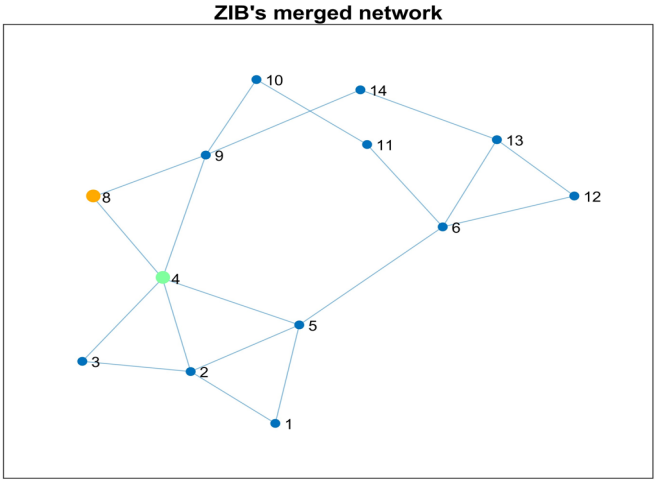

Figure 3. ZIB-merged IEEE 14-bus system with ZIB merged node (orange) and Node with PMU (green).

3.5. Firefly Algorithm Overview

The firefly algorithm is a swarm optimization technique inspired by tropical fireflies' behaviour in finding mating partners or their action of potential predator deterrence. This meta-heuristic algorithm is based on how fireflies interact with each other using their light-flashing body parts. This attraction of one firefly to another, the light intensity of each flash, and the distance-dependent nature of the algorithm have made it attractive in solving different optimization problems. The FA search model is such that the flashing light of each firefly and its intensity obey certain rules as in [39]. These rules are as follows:

1. In any given population of fireflies, they are all unisex, and, for mating purposes, any firefly will become attracted to a brighter firefly.
2. A firefly flies randomly if there is no brighter firefly than itself, otherwise, a less bright firefly flies towards a brighter one because the attractiveness of a less bright firefly is proportional to the light intensity of a brighter firefly, and both attractiveness and light intensity are inversely proportional to the distance from the light receptor.
3. The fitness function of the landscape determines the light intensity of each firefly.

3.6. Binary Firefly Algorithm (BFA)

In implementing the novel BFA shown by the pseudo code in Algorithm 1, a given firefly population of N_f, each i-th $\left(i = 1, 2, \ldots, N_f\right)$ firefly in the $X_i = (x_1, x_2, \ldots, x_i)$

position in the D-dimensional space represents a solution in a search space. In the BFA, a population of PMU placement candidates are generated from a symmetrical adjacency matrix $\boldsymbol{A}$ from a given N-bus system where any bus i $(i = 1, 2, \ldots, N)$ can have a PMU placed at its $X_i = (x_1, x_2, \ldots, x_N)$ position as part of the PMU placement set. The light intensity of each firefly becomes the degree centrality $C_D(i)$ of every bus. The degree centrality $C_D(i)$ is proportional to the search agent's attractiveness between any bus i and itself. The attractiveness β_{ij} of firefly i to firefly j is given by

$$\beta_{ij}(r_{ij}) = \beta_0 e^{-\gamma r_{ij}^2} \tag{8}$$

where (when the distance between any two fireflies is zero) the attractiveness is given by β_0 in the original FA; this attractiveness is the light intensity to the receptors of the observer firefly and the light absorption is represented by gamma (γ). To ensure that the search agent firefly i_{SF} will transverse the entire search space, $C_D(i)$ scores of all the busses in the system are ranked. The i_{SF} is assigned the value ψ given by

$$\psi = C_{D\_min}(i) - 0.01 \tag{9}$$

where $C_{D\_min}(i)$ is the lowest $C_D(i)$ score from the ranking of the buses. The $C_D(i)$ difference δ between the i_{SF} and any bus i is given by Equation (10), and this variable δ becomes the initial attractiveness β_0 in Equation (8) for BFA implementation.

$$\delta(i_{SF}) = C_D(i) - \psi \tag{10}$$

The Euclidean distance between i_{SF} to any bus i is represented by $r_{\theta i}$, which is expressed in Equation (11). In this paper, the distance the i_{SF} (initially at point θ) is from any bus i in the system is assumed to be arbitrary, and therefore it is set to unity.

$$r_{\theta i} = \sqrt{\sum_{d=1}^{D} (x_i - x_\theta)^2} = 1 \tag{11}$$

The i_{SF} attractiveness $\beta_{\theta i}$ to any bus i becomes:

$$\beta_{\theta i} = \delta(i)\exp(-\gamma) \tag{12}$$

Taking degree centrality $C_D(i)$ of a bus in position x_i and that of the i_{SF} in x_θ, the i_{SF} will move towards the bus in position x_i if and only if the $C_D(i)$ of the bus in position x_i is higher than that of i_{SF}. Once i_{SF} movement is achieved, a PMU placement with respect to the cases of consideration is carried out by changing a 0 bit to 1 bit in the index of bus i in the placement vector $\overline{Y}$. The system observability constraint function in (4) is evaluated at the new position. The i_{SF} movement is expressed by

$$x_\theta^{t+1} = x_\theta^t + \beta_\theta\left(x_i^t - x_\theta^t\right) + \alpha\varepsilon \tag{13}$$

where t is the iteration number, the $\beta_{\theta i}\left(x_j^t - x_i^t\right)$ term takes into consideration the attraction between i_{SF} and bus i. The adjacency matrices of the test cases used does not carry distance information between nodes; therefore, the step size α represents a single transition from the current node to the next desired node. The ε represents the bus random number achieved through the rand function in MATLAB applicable for the first iteration only when the i_{SF} considers the search space for the very first time, beyond which the ε is set to unity as the search trajectory becomes less random and highly objective. This process can terminate in one of the following ways:

1. System observability constraint function is satisfied or;

2. No bus $C_D(i)$ is greater than $C_D(i_{SF})$, leading to the completion of a local search by the i_{SF}, where x_b is the best solution given by Equation (14). However, the chances of the BFA reaching this point is rare as this will mean that the number of PMUs found is the same as N.

$$x_b = x_\theta^{t+1} = x_\theta^t + \alpha\varepsilon \tag{14}$$

Algorithm 1: Binary Firefly Algorithm

Input Variables: $A,\ d_i,\ t$
Initialize: δ *of* i_{SF} , $r_{\theta i},\ \gamma$
Output: *Optimal Placement set*
Randomly generate the initial population $X,\ X_i = (x_1, x_2, \ldots, x_i)$
Compute the Node degree of each bus by using (6)
Compute the Node degree centrality of each bus by using (7)
Compute $C_D(i)$ *difference* δ *between any bus* i *and* i_{SF} *using (10) as* $\delta = \{\delta_1, \delta_2 \ldots \delta_n\}$ *and initialize* ψ
while *t ≤ max iteration* ***do***
  for *i = 1* ***to*** *n* ***do***
    if $(C_D(i) > \psi)$ ***then***
      for *j = 1* ***to*** i ***do***
        Find max C_D
        Using (13) move i_{SF} *to bus* i
        Place a PMU at bus i
        Evaluate system Observability using (4)
      end for
      Rank buses without PMUs update i_{SF} *position*
    end if
  end for
  t = t + 1
end while
if *F(*$\bar{Y}$*)* ≥ $\bar{b}$ ***then***
  Rank Placement sets based on SORI and find the optimal placement set with the highest SORI
else
  Go to Step-5
end if
$x_b = x_\theta^{t+1}$
Stop.

4. Tests and Simulation Studies

The capability and robustness of the proposed BFA algorithm is tested on IEEE-14, 30, 39, 57, 118, 300, Polish 2383 and Polish 3120 from MATPOWER 8.0 b1 in MATLAB 2022b, running on an Intel(R), Xenon(R) CPU @3.30 Ghz, 3301 MHz 4 Core(s) CPU with a 16 GB RAM. The BFA deployed on these systems is on the following assumption. (1) The PMU technology used is the same throughout this study. (2) For all cases, the number of PMU channels is unlimited. (3) The communication network between GPS satellite and the PMU is under ideal conditions. The population size is within the range $N_f \in [14 - 3121]$ and the best setting of the light absorption (γ) coefficient is found to be 1. Throughout this paper,

the colour convention used to label PMU placement, ZIBs, bus and line measurement types follows Figure 4. The proposed BFA solves the OPP with consideration of the following measurements:

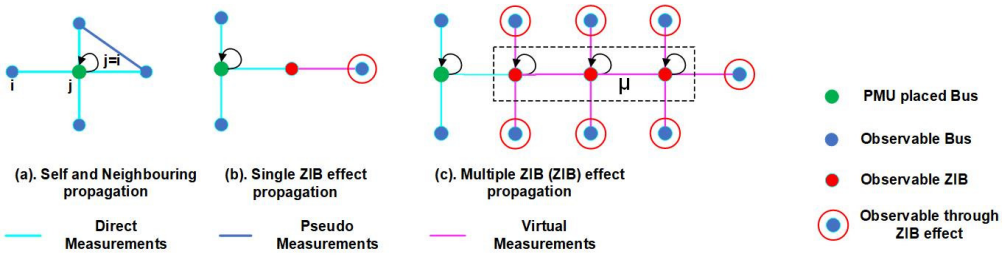

Figure 4. Colour conversion of measurement type.

1. Substation Measurements: These are measurements that are taken at the substation level by the PMU placed at that substation. In this paper, a power system is converted into an undirected graph; the self-propagations ($i = j$) signify this measurement.
2. Direct Measurements: These are measurements that are collected by PMU from all branches linked to the bus it is installed at, otherwise referred to as neighbouring propagations.
3. Pseudo Measurements: These kinds of measurements are voltage phasors and branch currents that are calculated from any two observable substations without PMUs installed on them.
4. Virtual Measurements: Essentially, these are measurements obtained through the effect of ZIBs. These measurements are possible through the following ways:
5. Single ZIB effect: One or more unobservable buses becoming observable through neighbouring an observable ZIB.
6. Group ZIB effect: Multiple unobservable buses become observable through neighbouring an interconnected group of observable ZIBs, forming a super node.

Adopted Observability Performance Metrics

Several bus observability performance metrics are proposed in the literature, all of which are aimed at calculating the risk of a bus becoming unobservable under contingencies. The authors of [40] introduced the concepts to look at incomplete observability, one of which is the Depth of Unobservability (DOU). DOU is defined as how many buses away an unobservable node is from the nearest observable bus in an incomplete observability state. This metric was not widely adopted as is noticeable from Table 1; however, in [28,41], the concept of DOU is complemented by proposing Observability Propagation Depth (OPD). OPD is defined as how many buses away the PMU is from the bus observed. OPD indicator ($\rho = 0$) signifies local PMU substation measurements; $\rho = 1$ indicates a direct observability of immediate nodes or substations that are neighbours to a PMU-installed bus through direct measurements or pseudo measurements if line impedances and incident branch current phasors are known. The ZIB effect makes it possible to have an increasing OPD indicator value as further buses become observable through a PMU installed a few buses away. The authors of [33] proposed Zero Injection Observation Depth (ZIOD) evaluated through a Zero Injection Influence Region (ZIIR) or a super node (S), as proposed in [28]. The ZIIRs are shown in Figure 5 as μ_1 and μ_2, allowing seven PMUs to be purely observable through the ZIB effect only. ZIOD is a ZIB effect-specific metric form of OPD that is defined as the observability depth (how many ZIB buses from a PMU-installed bus) due to the ZIB effect propagation of the bus being observed by a PMU to which the whole ZIIR is observable. ZIB effect utilization reduces the number of PMUs to be installed. To determine how useful ZIBs are in optimal PMU number reduction in any given EPS, the authors of [33] further proposed yet another metric, the Zero Injection Utilization Rate (ZIUR). ZIUR is defined as

the total number of buses observable through a PMU connected to an observable ZIB or ZIIR region (ZIB effect) divided by Z_T in an EPS, and this is given by:

$$\text{ZIUR} = \frac{\sum_{i \in \boldsymbol{B}} (1 - y_i)}{|Z_T|} \times 100\%. \tag{15}$$

where Z_T is the total number of ZIBs in the EPS, and if $1 - y_i$ yields 1, then bus i quantities are measured through the ZIB effect. It has been found in [42,43] that for a particular optimal PMU placement solution, placement may exist with the same number of PMUs but in different locations. This gives rise to the node uniqueness which each node connectivity brings into the search space. Node connectivity information like node degree centrality relates directly to how many times a node is observed by other nodes connected to it; this defines the Bus Observability Index (*BOI*) expressed in (16):

$$BOI = a_{(n \times n)} \cdot N_{PMU}^{T} \tag{16}$$

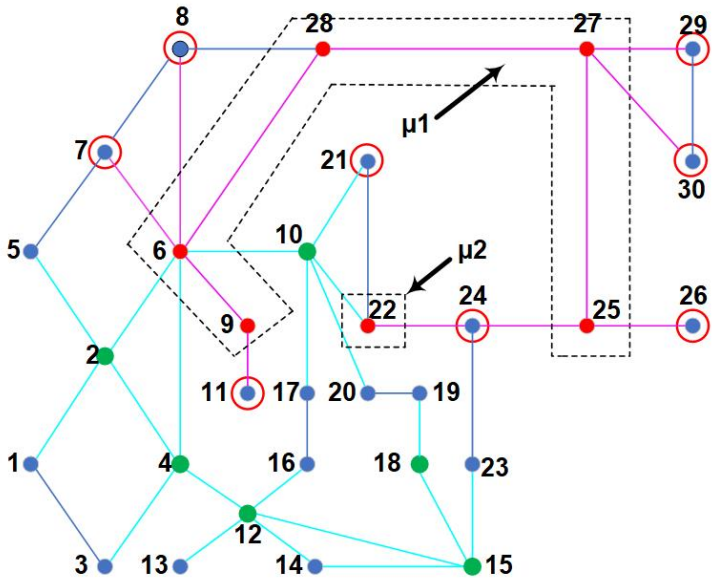

Figure 5. Zero Injection Influence Region illustration using IEEE 30-bus indicating nodes with no PMUs placed (blue), PMU placed (green), ZIB nodes (red) and node observed through ZIB effect in a (red cycle), and lines with direct (cyan), pseudo (blue) and virtual (violet) measurements.

The sum of bus observability scores of all the buses in each system is defined as the System Observability Redundancy Index (*SORI*) and is given by:

$$SORI = \sum_{i=1}^{N_{PMU}} a_{(n \times n)} \cdot N_{PMU}^{T} \tag{17}$$

where, a represents elements in an adjacency matrix of a given system, and N_{PMU} is the number of PMUs given by the total observability placement set.

5. Illustrative Results and Discussions

The bus network data of these test cases are shown in Table 2. Information on buses IEEE 300-bus, Polish 2383 and Polish 3120 have been omitted.

Table 2. Test cases specification.

IEEE-Bus System	ZIB Locations	Radial Buses Locations	Bus with the Maximum Number of Branches
14-Bus	7	8	4
30-Bus	6, 9, 22, 25, 27, 28	11, 13, 26	6
39-Bus	1, 2, 5, 6, 9, 10, 11, 13, 14, 17, 19, 22	30, 31, 32, 33, 34, 36, 37, 38	16
57-Bus	4, 7, 11, 21, 22, 24, 26, 34, 36, 37, 39, 40, 45, 46,48	33	9
118-Bus	5, 9, 30, 37, 38, 63, 64, 68, 71, 81	10, 73, 87, 111, 112, 116, 117	49

BFA algorithm is tested in case studies. The visualization follows the colour code of Figures 5 and 6. For each case, the presentation is such that the PMU placement sets, along with the necessary observability performance indices and computational time, are in a table, followed by a placement plot of the IEEE 30-bus for an easy comparison between cases and a convergence curve of one of the test cases.

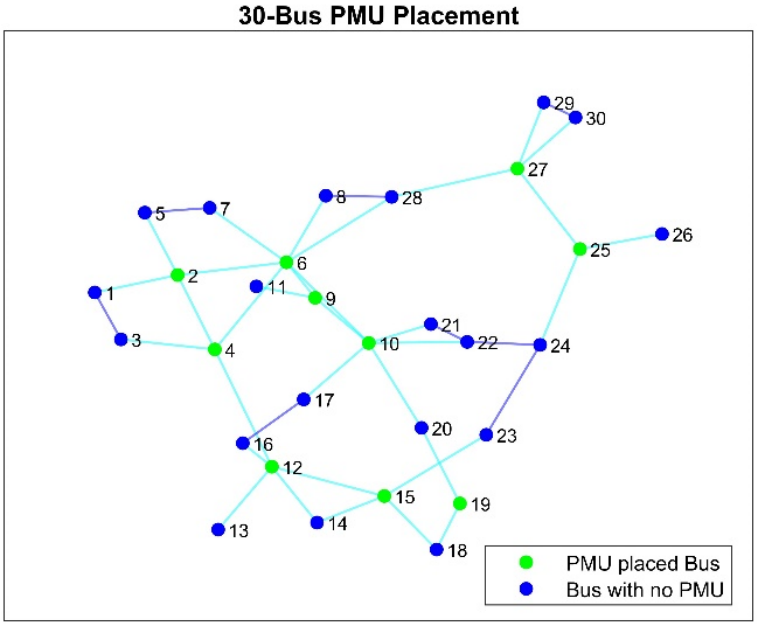

Figure 6. Normal operation 30-bus placement. indicating nodes with no PMUs placed (blue), PMU placed (green) and lines with direct (cyan) and pseudo (blue) measurements.

5.1. Case 1: Normal Operation without ZIB Effect and Unlimited Channel Limits

This case study considers achieving complete network observability under direct and pseudo-PMU measurement only. Table 3 shows PMU placement results for each test case against their performance indices. The BFA managed to find many different PMU solution sets as recorded in Table 3. Out of all solution sets that have been found with the same optimal number of PMUs, the bold PMU placement set is the one that has the best SORI value. Clear achievements of the algorithm from Table 3 show that the results obtained are the same as those achieved in [6,24] in terms of BOI and SORI. Figure 6 shows the optimal PMU placement on IEEE Bus-30 using the proposed BFA. Notice that this optimal PMU placement map has PMUs on buses with the highest degree centrality scores. This strategy evades radial buses based on their low degree centrality scores, as well as reducing the numbers of installed PMUs. Figure 7 shows the convergence curve of the proposed

BFA on the IEEE-57 bus system; the algorithm took longer on 18 PMU placement sets but demonstrates the ability to escape the local minima as it manages to find the global minima of 17 PMU placement sets, which is consistent with the findings of existing methods.

Table 3. PMU locations for normal operation without ZIB effect.

IEEE Test System	Optimal Number of PMUs	Optimal PMU Locations	Best BOI from Placement Sets	Maximum Redundancy	Best SORI	CPU Time
14-bus	4	2, 6, 7, 9	1, 1, 1, 3, 2, 1, 2, 1, 2, 1, 1, 1, 1, 1	3	19	0.847 s
30-bus	10	2, 4, 6, 9, 10, 12, 15, 19, 25, 27. 1, 7, 9, 10, 12, 18, 24, 25, 27, 28. 1, 2, 6, 9, 10, 12, 15,20, 25, 29.	1, 3, 1, 4, 1, 5, 1, 1, 3, 3, 1, 3, 1, 2, 2, 1, 1, 2, 1, 2, 1, 1, 1, 1, 2, 1, 2, 2, 1, 1	5	52	0.761 s
39-bus	13	2, 6, 9, 10, 13, 14, 17, 19, 20, 22, 23, 25, 29. 2, 6, 9, 10, 12,14,17,19, 20, 22, 23, 25, 29.	1, 2, 1, 1, 1, 1, 1, 1, 1, 2, 2, 1, 3, 2, 1, 2, 1, 1, 2, 2, 1, 2, 2, 1, 2, 2, 1, 1, 1, 1, 1, 1, 1, 1, 1, 1, 1, 1, 1	3	52	1.418 s
57-bus	17	1, 4, 9, 15, 20, 24, 26, 28, 29, 31, 32, 36, 38, 41, 47, 51, 53, 57. 1, 4, 9, 20, 22, 25, 26, 29, 32, 36, 39, 41, 45, 46, 49, 51, 53.	2, 1, 2, 1, 1, 1, 1, 1, 1, 2, 2, 1, 2, 1, 2, 1, 1, 2, 1, 1, 1, 1, 1, 1, 2, 1, 1, 2, 2, 1, 2, 1, 1, 1, 1, 1, 2, 1, 1, 1, 1, 1, 1, 1, 1, 1, 1, 2, 1, 1, 1, 2, 1, 1, 1, 2, 1	2	72	3.892 s
118-bus	32	2, 6, 9, 11, 12, 17, 21, 24, 26, 28, 34, 37, 41, 45, 49, 52, 56, 62, 64, 68, 71, 75, 77, 80, 85, 86, 91, 94, 101, 104, 107, 108, 110, 114	1, 2, 3, 1, 1, 1, 1, 2, 1, 1, 3, 1, 1, 1, 2, 2, 1, 1, 1, 1, 1, 1, 2, 1, 1, 1, 2, 1, 1, 1, 1, 1, 1, 2, 1, 1, 2, 1, 1, 2, 1, 3, 1, 1, 2, 1, 1, 1, 4, 1, 2, 1, 1, 3, 1, 1, 1, 1, 2, 1, 2, 1, 1, 1, 2, 3, 1, 1, 4, 3, 1, 2, 1, 1, 2, 1, 4, 1, 1, 2, 2, 1, 1, 1, 2, 2, 1, 1, 3, 1, 1, 2, 1, 1, 1, 2, 1, 1, 1, 1, 1, 1, 2, 1, 1, 1, 1, 1, 1, 1, 1, 1, 1, 1, 1, 1, 1, 1	4	164	2896.1 s
300-bus	91	1, 2, 3, 11, 12, 15, 17, 20, 22, 23, 25, 29, 31, 33, 35, 36, 37, 38, 43, 48, 49, 53, 54, 55, 58, 59, 60, 62, 64, 65, 71, 79, 83, 85, 86, 88, 89, 90, 98, 99, 101, 103, 109, 111, 112, 113, 116, 118, 119, 124, 132, 133, 138, 143, 145, 152, 157, 163, 167, 173, 175, 177, 183, 185, 189, 190, 193, 196, 198, 199, 203, 204, 208, 210, 211, 213, 216, 217, 219, 224, 225, 228, 267, 268, 269, 270, 272, 273, 274, 276, 294	2, 2, 3, 2, 1, 1, 2, 3, 1, 2, 1, 1, 1, 1, 3, 1, 1, 1, 1, 2, 2, 3, 2, 2, 1, 1, 1, 1, 3, 1, 1, 1, 1, 1, 1, 4, 3, 2, 3, 1, 2, 2, 1, 1, 1, 1, 2, 2, 3, 1, 1, 1, 2, 2, 2, 2, 1, 2, 3, 3, 2, 1, 1, 3, 2, 1, 1, 2, 1, 1, 1, 1, 2, 1, 1, 1, 1, 1, 1, 1, 1, 1, 3, 1, 2, 1, 1, 2, 1, 1, 1, 1, 1, 1, 1, 1, 1, 2, 2, 2, 2, 1, 1, 1, 2, 1, 2, 2, 2, 1, 2, 1, 2, 1, 1, 3, 2, 1, 2, 1, 1, 2, 1, 1, 1, 1, 1, 1, 2, 1, 1, 2, 1, 2, 1, 1, 2, 1, 1, 1, 1, 1, 2, 1, 1, 1, 2, 1, 1, 1, 2, 1, 1, 1, 1, 2, 2, 1, 1, 1, 1, 1, 2, 1, 1, 2, 1, 1, 3, 1, 1, 1, 1, 1, 1, 1, 1, 1, 1, 1, 1, 1, 2, 1, 2, 1, 2, 1, 2, 2, 2, 1, 2, 3, 1, 1, 1, 3, 2, 1, 1, 1, 1, 1, 1, 1, 3, 1, 1, 3, 2, 1, 2, 2, 1, 3, 1, 1, 1, 1, 1, 1, 2, 2, 1, 1, 1, 1, 1, 1, 1, 1, 1, 1, 1, 1, 1, 1, 1, 1, 1, 1, 1, 1, 1, 1, 1, 1, 1, 1, 1, 1, 1, 1, 1, 1, 1, 1, 1, 1, 1, 1, 1, 1, 1, 2, 4, 2, 1, 2, 3, 2, 3, 3, 1, 2, 1, 1, 1, 1, 1, 1, 1, 1, 1, 1, 1, 1, 1, 1, 2, 1, 1, 2, 1, 1, 1, 1, 1, 1	4	465	4320.2 s

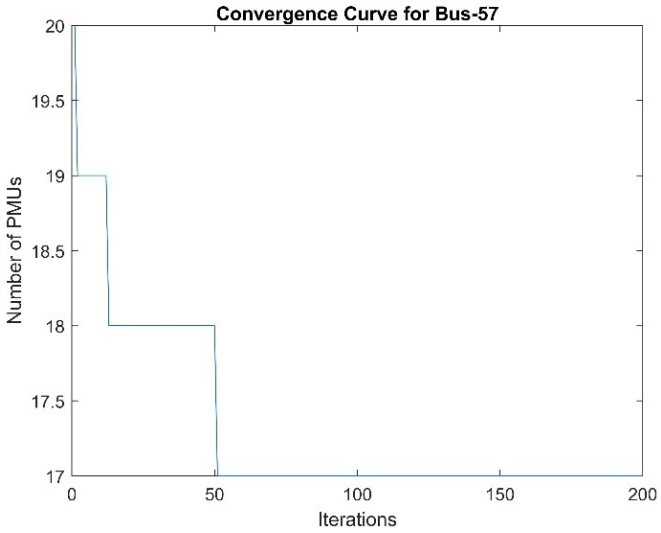

Figure 7. 57-Bus convergence curve.

5.2. Case 2: Normal Operation with ZIB Effect Consideration

Observability through the ZIB effect can drastically reduce the number of PMUs in an EPS. In Table 4, the PMU numbers have declined from what was required to make the test systems observable. But how safe and reliable is such an arrangement of sensors? SORI values also show a decline, which signifies a very low redundancy and reliability in any system. In Figure 8, bus 29 can be observed by PMUs installed on buses 2, 4 and 10 through ZIIR containing buses 9, 6, 28, 27, and 25. Even though there is no current injection through the ZIIR, there must be a continuity, as each line current and voltage of each bus are important state variables that ensure bus 29 or any other bus which is observable through the same ZIIR to remain observable. This is a great threat to the observability of the entire system.

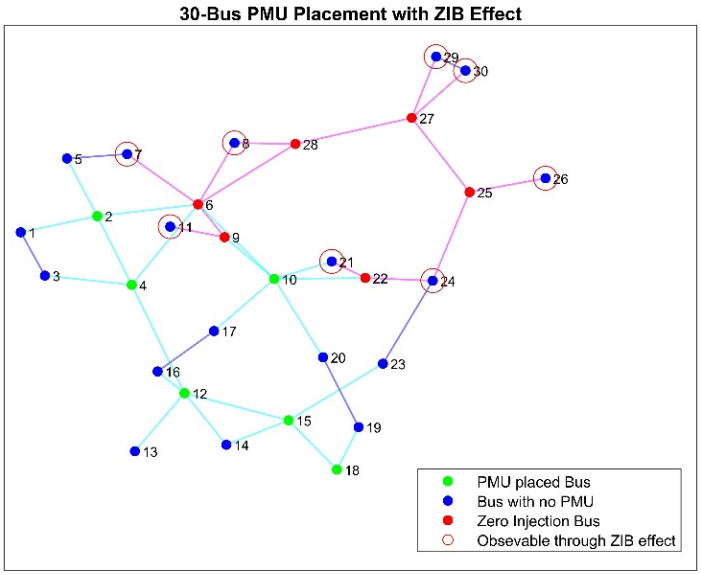

Figure 8. Normal operation 30-bus placement with ZIB effect indicating nodes with no PMUs placed (blue), PMU placed (green), ZIB nodes (red) and node observed through ZIB effect in a (red cycle), and lines with direct (cyan), pseudo (blue) and virtual (violet) measurements.

Table 4. Normal operation with ZIB effect consideration.

IEEE Test System	Optimal Number of PMUs	Optimal PMU Locations	Best BOI from Placement Sets	Maximum Redundancy	Best SORI	CPU Time
14-bus	3	2, 6, 9	1, 1, 1, 2, 2, 1, 1, 1, 1, 1, 1,1, 1	2	15	2.58 s
30-bus	6	2, 4, 10, 12, 15, 20. 2, 4, 8, 10, 13, 17. 2, 4, 8, 10, 13, 16. 1, 6, 8, 10, 13, 16. 3, 5, 8, 10, 16, 20. 2, 4, 8, 10, 13, 18. 3, 5, 8, 10, 13, 16.	1, 3, 1, 4, 1, 3, 3, 4, 3, 3, 1, 2, 2, 1, 1, 1, 1, 2, 1, 1, 3, 3, 3, 3	4	51	3.04 s
39-bus	7	1, 8, 16, 20, 23, 25, 29. 1, 5, 11, 13, 15, 17, 19. 1, 5, 9, 11, 13, 15, 19. 1, 5, 10, 11, 13, 15,19.	2, 2, 1, 1, 1, 1, 1, 2, 2, 1, 2, 2, 1, 2, 2, 2, 1, 1, 1, 2, 1, 1, 2, 1, 1, 1, 1, 1, 1	2	40	2.64 s
57-bus	12	1, 9, 10, 15, 18, 20, 25, 29, 32, 49, 53, 56. 1, 7, 8, 12, 15, 17, 19, 22, 25, 34, 38, 41. 1, 8, 12, 15, 17, 19, 22, 25, 31, 34, 39, 41. 1, 4, 7, 8, 12, 16, 19, 22, 25, 34, 38, 41.	2, 1, 2, 1, 2, 2, 2, 2, 2, 3, 1, 2, 1, 1, 1, 2 , 1, 2, 1, 1, 1, 1, 1, 1, 1, 1, 2, 3, 2, 1, 1, 1, 1, 1, 1, 1, 2, 1, 1, 1, 1, 1	2	59	2.73 s
118-bus	28	3, 8, 12, 15, 19, 21, 27, 31, 32, 34, 42, 45, 49, 53, 56, 62, 72, 75, 77, 80, 83, 86, 89, 92, 96, 100, 105, 110 3, 7, 10, 13, 17, 19, 25, 28, 29, 31, 37, 40, 44, 48, 51, 57, 63, 66,68, 71,73, 76,79, 82,86, 90, 95, 100	1, 1, 3, 2, 2, 1, 3, 1, 3, 2, 1, 2, 2, 1, 4, 1, 3, 2, 1, 1, 1, 1, 1, 2, 2, 1, 1, 2, 3, 3, 3, 2, 1, 2, 3, 1, 2, 1, 1, 2, 1, 1, 1, 3, 1, 1, 1, 1, 3, 1, 1, 1, 1, 1, 1, 1, 1, 3, 2, 1, 4, 2, 1, 1, 1, 2, 1, 3, 1, 1, 3, 3, 1, 1, 3, 1, 1, 1, 2, 1, 1, 3, 1, 3, 1, 2, 2, 2, 2, 2, 1, 1, 3, 2, 1, 2, 1, 1, 1, 1, 1, 1, 1, 1, 1, 1, 1	4	174	440.50 s
300-bus	65	1, 2, 3, 11, 14, 17, 22, 25, 26, 37, 38, 42, 43, 48, 49, 53, 55, 58, 59, 60, 64, 76, 77, 80, 85, 88, 91, 92, 98, 99, 104, 118, 121, 124, 125, 131, 133, 136, 140, 141, 155, 158, 160, 163, 167, 169, 171, 177, 183, 185, 193, 196, 202, 208, 210, 211, 213, 217, 225, 228, 267, 268, 269, 274, 294	2, 2, 11, 2, 2, 3, 1, 2, 1, 1, 1, 11, 1, 1, 2, 1, 1, 2, 2, 2, 9, 4, 1, 1, 10, 3, 10, 2, 2, 1, 1, 1, 1, 2, 2, 3, 1, 1, 9, 10, 2, 3, 10, 10, 9, 9, 1, 1, 1, 1, 1, 1, 1, 2, 2, 1, 2, 3, 1, 2, 1, 1, 2, 1, 1, 1, 1, 1, 2, 2, 2, 1, 2, 1, 1, 1, 3, 2, 1, 1, 3, 2, 1, 3, 1, 1, 11, 2, 2, 1, 1, 1, 1, 2, 1, 2, 1, 1, 1, 1, 1, 1, 1, 1, 1, 1, 1, 3, 1, 1, 1, 1, 1, 1, 1, 1, 1, 1, 1, 2, 1, 1, 3, 1, 1, 2, 1, 1, 1, 1, 1, 1, 1, 2, 1, 1, 1, 1, 10, 1, 1, 10, 1, 9, 9, 2, 1, 9, 1, 2, 1, 1, 3, 2, 1, 11, 2, 1, 9, 2, 1, 1, 1, 9, 1, 1, 1, 1, 1, 1, 1, 1, 1, 1, 1, 1, 1, 1, 1, 1, 1, 1, 1, 9, 1, 9, 1, 1, 1, 1, 1, 1, 1, 1, 1, 1, 9, 1, 1, 1, 1, 1, 9, 1, 1, 1, 1, 4, 4, 2, 2, 1, 1, 1, 1, 1, 1, 1, 1, 1, 1, 1, 1, 1, 1, 1, 3, 3, 3, 3, 3, 3, 3, 3, 1	11	528	1845 s

The phasor network has increased the chances of failure even though the cost of PMU installations is lower than in case 1. Another significant observation is on the observability of lines made possible through direct measurements and pseudo measurements. With regard to direct measurements, let us observe edges emanating from node 6, which is cyan in colour, in Figure 6. In Figure 8, node 6 is one of the ZIBs in IEEE 30-bus, therefore in considering the effect of ZIBs, the branch current of the edges 6–7, 6–8, 6–9 and 6–28 becomes observable though virtual measurement. The ZIB effect has increased the state variables needed to make these edges observable. The same effect is seen with pseudo measurement, some lines that were observable through pseudo measurements in Figure 6 (the blue edges 21–22, 22–24 and 6–28) have become observable through virtual measurements in Figure 8. This shows that observability through the ZIB effect further jeopardizes the system's observability should there be a loss of even a line measurement in the ZIIR. In

the convergence curve of IEEE 118-Bus shown in Figure 9, the BFA takes less time to solve the OPP for the optimal placement sets with 28 PMUs. This can also be seen in comparing the computational times of IEEE 118-Bus in Tables 3 and 4. Considering the ZIB effect also reduces the number of possible optimal PMU placement solution sets.

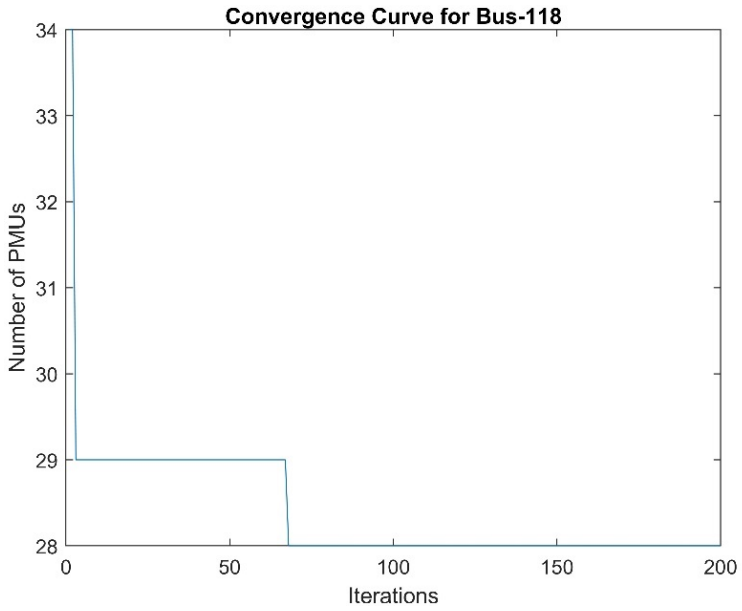

Figure 9. 118-Bus convergence curve under consideration of ZIB effect.

5.3. Case 3: Single PMU Outage

In a case where PMU malfunctions and drops out of the phasor network due to communication link failure, CT and VT failures, and GPS synchronization signal loss, the possibilities of faults occurring at an unmonitored substation increases. As already mentioned, PMUs play a paramount role in the observability of the EPS. Table 5 shows how BFA has performed in solving the OPP problem under a single PMU loss consideration. The validity of BFA performance in satisfying PMU placement constraint that ensures each bus is observed by at least two PMUs is seen through the BOI entry of every bus in Table 5. PMU placement aimed at robustness against a single PMU loss in the phasor network carries a significant trade-off between the cost and reliability of system observability. When comparing the case 1 and case 2 PMU placement sets of 14-bus with case 3 results, in case 3, the optimal number of PMUs has more than doubled the number of PMUs in case 1 and tripled that of case 2. This means that the price of installation has more than doubled from cases 1 and 2, but this comes at the greatest benefit of having most buses being observed by a PMU through direct and local substation measurements. The key indicator for this in Table 5 is the highest values of SORI achieved for each test system thus far. Observability through PMUs is reliable since there are fewer state variables to keep a particular bus observable, but the cost of installation has surged. Another distinctive advantage is that if Figure 10 is compared with Figures 6 and 8, in Figure 10, IEEE 30-bus shows that there are no pseudo measurements, which is good for the system observability because fewer measurements leading to the observability of any bus improves the measurement redundancy of the system.

Table 5. Single PMU loss.

IEEE Test System	Optimal Number of PMUs	Optimal PMU Locations	Best BOI	Maximum Redundancy	SORI	CPU Time
14-bus	9	2, 4, 5, 6, 7, 8, 9, 11, 13.	2, 3, 2, 5, 4, 4, 4, 2, 3, 2, 2, 2, 2, 2	4	39	0.79 s
30-bus	21	2, 3, 4, 6, 7, 9, 10, 11, 12, 13, 15, 17, 19, 20, 22, 24, 25, 26, 27, 28, 30.	2, 3, 2, 5, 2, 7, 2, 2, 4, 6, 2, 4, 2, 2, 2, 2, 2, 2, 2, 3, 2, 3, 2, 3, 4, 2, 4, 3, 2, 2	7	85	0.73 s
39-bus	28	2, 3, 6, 8, 9, 10, 11, 13, 14, 16, 17, 19, 20, 22, 23, 25, 26, 29, 30, 31, 32, 33, 34, 35, 36, 37, 38, 39	2, 4, 2, 2, 2, 3, 2, 2, 3, 4, 3, 2, 3, 2, 2, 3, 2, 2, 4, 3, 2, 3, 3, 2, 4, 3, 2, 2, 3, 2, 2, 2, 2, 2, 2, 2, 2, 2, 2	4	96	0.83 s
57-bus	36	1, 3, 4, 6, 9, 10, 11, 12, 14, 15, 18, 20, 21, 22, 24, 25, 27, 28, 29, 31, 32, 33, 35, 36, 37, 38, 41, 45, 47, 48, 49, 51, 53, 54, 56, 57	2, 2, 3, 5, 2, 2, 2, 2, 4, 4, 3, 3, 6, 2, 5, 2, 2, 3, 2, 2, 3, 3, 2, 3, 3, 2, 2, 3, 2, 2, 2, 3, 2, 2, 2, 3, 3, 5, 2, 2, 3, 2, 2, 2, 2, 2, 2, 4, 3, 2, 2, 2, 2, 2, 2, 3, 2	6	148	1.1 s
118-bus	68	2, 3, 5, 7, 9, 10, 11, 12, 15, 17, 19, 21, 22, 24, 25, 27, 29, 30, 31, 32, 34, 36, 37, 40, 42, 44, 45, 46, 49, 51, 53, 54, 56, 57, 59, 62, 64, 65, 66, 68, 70, 71, 73, 75, 77, 79, 80, 83, 85, 86, 87, 89, 90, 92, 94, 96, 100, 102, 105, 106, 109, 110, 111, 112, 115, 116, 117, 118	2, 2, 3, 2, 3, 2, 2, 3, 2, 2, 3, 6, 2, 2, 3, 2, 4, 2, 3, 2, 2, 2, 4, 2, 2, 2, 4, 2, 2, 2, 4, 3, 2, 4, 2, 2, 3, 3, 2, 3, 2, 4, 2, 2, 4, 2, 2, 2, 9, 2, 2, 2, 2, 6, 3, 5, 2, 2, 4, 2, 3, 2, 2, 2, 4, 5, 2, 3, 5, 4, 3, 2, 2, 2, 4, 2, 4, 2, 2, 5, 2, 3, 2, 2, 4, 3, 2, 2, 6, 3, 2, 6, 2, 4, 2, 3, 2, 2, 2, 4, 2, 2, 3, 2, 2, 3, 2, 2, 2, 4, 2, 2, 2, 2, 2, 2, 2, 2	9	323	3.72 s
300-bus	204	1, 2, 3, 5, 7, 8, 11, 12, 15, 16, 17, 19, 20, 22, 23, 25, 27, 29, 31, 33, 35, 36, 37, 38, 39, 41, 43, 44, 47, 48, 49, 51, 53, 54, 55, 57, 58, 59, 60, 62, 64, 65, 68, 69, 71, 73, 78, 79, 81, 82, 83, 84, 85, 86, 87, 88, 89, 90, 93, 97, 98, 99, 100, 101, 102, 103, 105, 109, 111, 112, 113, 115, 116, 118, 119, 122, 124, 125, 132, 134, 135, 137, 138, 143, 144, 145, 148, 149, 150, 152, 153, 155, 157, 158, 160, 162, 163, 164, 167, 168, 171, 173, 175, 177, 179, 183, 184, 185, 189, 190, 192, 193, 194, 196, 198, 199, 201, 202, 203, 204, 206, 208, 209, 210, 211, 212, 213, 215, 216, 217, 218, 219, 220, 223, 224, 225, 228, 229, 230, 231, 232, 233, 234, 235, 236, 237, 238, 239, 240, 241, 242, 243, 244, 247, 248, 249, 250, 251, 252, 253, 254, 255, 256, 257, 258, 259, 260, 261, 262, 263, 264, 265, 267, 268, 269, 270, 272, 273, 274, 275, 276, 277, 278, 279, 280, 281, 282, 283, 284, 285, 286, 287, 288, 289, 290, 292, 293, 294, 295, 296, 297, 298, 299, 300	4, 4, 5, 2, 3, 2, 4, 3, 2, 2, 3, 4, 2, 2, 4, 3, 3, 2, 2, 4, 2, 3, 5, 2, 2, 2, 2, 2, 3, 2, 4, 4, 3, 2, 6, 4, 2, 6, 3, 3, 2, 2, 5, 3, 2, 2, 3, 4, 4, 2, 2, 2, 4, 3, 3, 2, 2, 3, 4, 5, 3, 4, 2, 6, 3, 3, 2, 3, 2, 2, 3, 2, 3, 2, 2, 2, 2, 2, 5, 2, 5, 3, 5, 3, 4, 4, 3, 4, 4, 4, 2, 2, 2, 2, 2, 2, 3, 5, 3, 3, 2, 3, 2, 3, 4, 2, 2, 3, 3, 2, 4, 4, 2, 2, 2, 6, 2, 2, 4, 3, 2, 2, 2, 4, 3, 2, 3, 2, 2, 2, 2, 2, 2, 3, 2, 3, 3, 2, 2, 2, 2, 2, 2, 2, 3, 2, 2, 3, 2, 2, 3, 3, 2, 3, 2, 2, 2, 2, 2, 2, 2, 2, 3, 2, 2, 2, 2, 2, 3, 2, 2, 2, 4, 2, 2, 3, 3, 2, 2, 2, 2, 2, 2, 3, 2, 2, 2, 2, 5, 3, 2, 2, 3, 2, 2, 3, 3, 4, 3, 2, 2, 2, 3, 3, 2, 2, 3, 2, 2, 4, 3, 2, 3, 2, 2, 6, 3, 2, 2, 2, 2, 2, 2, 2, 3, 2, 2, 2, 2, 2, 2, 2, 2, 2, 2, 2, 2, 2, 2, 2, 2, 2, 2, 2, 2, 2, 2, 2, 2, 2, 2, 2, 2, 2, 2, 2, 2, 2, 2, 2, 2, 2, 2, 2, 2, 2, 2, 2, 3, 5, 10, 4, 6, 3, 4, 4, 4, 2, 4, 2, 2, 2, 2, 2, 2, 2, 2, 2, 2, 2, 2, 2, 2, 2, 2, 2, 3, 2, 2, 2, 2, 2, 2	10	788	69.29 s

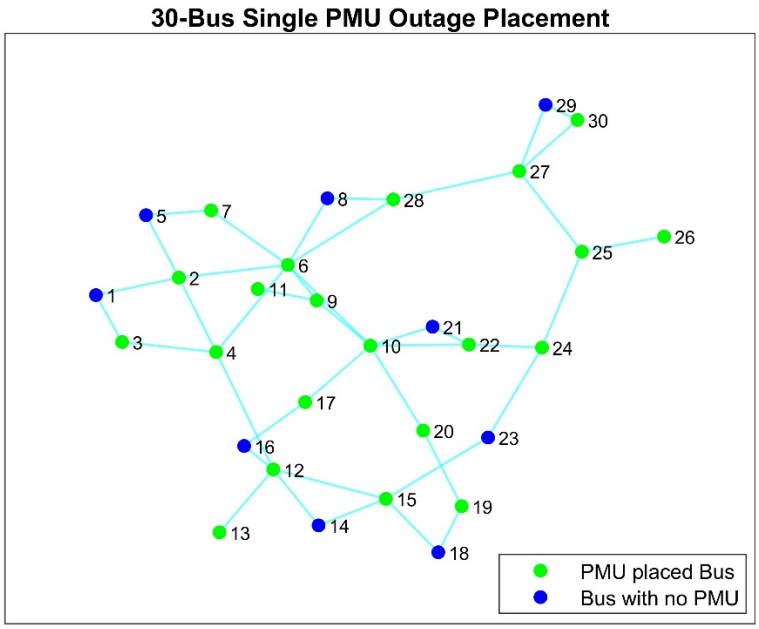

Figure 10. 30-Bus single PMU outage indicating nodes with no PMUs placed (blue), PMU placed (green) and lines with direct (cyan) and pseudo (blue) measurements.

5.4. Case 4: Single PMU Outage with ZIB Effect

This case study is the extension of case 3 as it implements the use of the ZIB effect as a PMU reduction strategy after achieving observability under the PSO observability constraint covered. As expected, when introducing the ZIB effect under a single PMU loss contingency, there is a notable reduction in PMUs. The same arguments made under case 2 regarding reduced reliability and measurement redundancy still hold. Case 3 eroded most of those concerns, resulting in increased PMU installation costs. Single PMU loss with ZIB effect strikes a balance between reliability and the cost outlay of phasor network sensing infrastructure. If we consider the IEEE 30-bus system in Case 2, the number of optimal PMUs is six, and as already pointed out, the system is fragile and sensitive as a single fault can lead to the loss of the observability of many buses. In case 3, still in IEEE 30-bus, the system had 21 PMUs, making it observable; it is costly but robust, as direct measurement reduces state variables for any bus to be observable. In Table 6, the IEEE 30-bus system has 12 optimal number PMUs as seen in Figure 11. Every bus can be seen by at least two PMUs, either by direct measurement or through the ZIB effect. These results show that when the BFA solves the OPP for SPO with ZIB effect, while considering the trade-offs outlined, case 4 presents the middle ground for both PMU installation costs, as shown in the reduced PMU number from case 3 in Table 7 and the good reliability, as there are still no pseudo measurements under complete observability of the EPS through the phasor network when comparing Figures 10 and 11.

Table 6. Single PMU loss with ZIB effect.

IEEE Test System	Optimal Number of PMUs	Optimal PMU Locations	Best BOI	Maximum Redundancy	SORI	CPU Time
14-bus	7	2, 4, 5, 6, 9, 11, 13	2, 3, 2, 4, 4, 4, 2, 2, 2, 2, 2, 2, 2	4	33	1.38 s
30-bus	12	2, 4, 5, 6, 9, 11, 13, 15, 17, 19, 20, 24	2, 5, 2, 7, 2, 5, 5, 7, 5, 4, 2, 2, 2, 2, 2, 2, 2, 3, 2, 2, 5, 5, 5, 5	5	85	1.63 s
39-bus	16	1, 3, 8, 15, 16, 20, 21, 23, 25, 26, 29, 34, 36, 37, 38, 39	4, 3, 3, 2, 2, 2, 2, 3, 4, 2, 3, 3, 3, 2, 5, 3, 2, 2, 3, 3, 2, 2, 2, 2, 2, 2, 2, 2, 2	5	74	1.74 s
57-bus	23	1, 3, 6, 9, 10, 12, 13, 15, 18, 20, 25, 27, 29, 31, 32, 33, 38, 41, 49, 51, 53, 54, 56	2, 2, 4, 3, 4, 3, 5, 4, 4, 6, 2, 4, 2, 2, 3, 2, 2, 4, 2, 2, 2, 2, 2, 2, 3, 2, 3, 4, 4, 2, 3, 2, 2, 3, 2, 2, 2, 2, 2, 2, 3, 2	6	115	2.0 s
118-bus	60	2, 3, 6, 8, 10, 11, 12, 15, 17, 19, 21, 22, 26, 27, 29, 31, 32, 34, 35, 40, 42, 44, 45, 46, 49, 51, 53, 54, 56, 57, 59, 62, 65, 66, 70, 72, 75, 77, 79, 80, 83, 85, 86, 87, 89, 91, 92, 94, 96, 100, 102, 105, 106, 109, 110, 111, 112, 115, 117, 118	2, 2, 5, 4, 4, 2, 11, 2, 5, 5, 2, 2, 3, 2, 9, 2, 3, 2, 2, 2, 2, 2, 2, 7, 3, 2, 2, 4, 3, 8, 8, 7, 2, 7, 8, 2, 3, 2, 2, 4, 2, 2, 2, 6, 2, 2, 2, 2, 5, 3, 4, 2, 2, 4, 2, 3, 2, 10, 4, 2, 6, 3, 2, 2, 2, 4, 2, 3, 2, 2, 5, 3, 2, 2, 4, 3, 2, 2, 3, 2, 2, 6, 2, 4, 2, 3, 2, 2, 2, 4, 2, 2, 3, 2, 2, 3, 2, 2, 2, 4, 2, 2, 2, 2, 2, 2, 2, 2	11	339	4.44 s
300-bus	143	1, 2, 3, 5, 8, 11, 15, 17, 19, 20, 22, 25, 27, 31, 37, 38, 41, 43, 44, 47, 48, 49, 51, 53, 55, 58, 59, 60, 64, 66, 78, 79, 83, 84, 85, 86, 87, 88, 89, 90, 93, 98, 99, 101, 103, 105, 115, 116, 118, 119, 122, 124, 125, 132, 134, 135, 136, 141, 152, 155, 157, 158, 160, 162, 163, 164, 167, 168, 169, 171, 175, 177, 179, 184, 185, 190, 192, 193, 194, 196, 199, 202, 203, 204, 206, 208, 209, 210, 211, 212, 213, 215, 217, 218, 224, 225, 228, 229, 230, 232, 233, 235, 236, 237, 238, 239, 241, 243, 244, 247, 248, 249, 250, 252, 253, 256, 257, 258, 259, 260, 262, 264, 265, 267, 268, 269, 274, 275, 277, 279, 280, 281, 282, 283, 284, 285, 286, 287, 288, 289, 290, 294, 300	4, 4, 23, 6, 6, 3, 2, 6, 3, 2, 2, 16, 3, 2, 9, 2, 3, 2, 2, 2, 14, 6, 3, 2, 17, 2, 18, 2, 2, 4, 2, 2, 2, 3, 4, 4, 2, 2, 16, 16, 3, 4, 16, 17, 14, 17, 3, 2, 2, 2, 2, 2, 2, 5, 4, 2, 8, 6, 3, 4, 4, 2, 3, 3, 3, 2, 2, 2, 2, 3, 4, 2, 2, 2, 3, 2, 7, 6, 2, 2, 9, 2, 2, 4, 3, 2, 15, 4, 3, 2, 3, 2, 2, 2, 2, 3, 2, 3, 3, 2, 3, 3, 5, 5, 5, 2, 2, 3, 2, 2, 2, 2, 2, 2, 2, 2, 2, 2, 2, 2, 2, 4, 4, 2, 2, 5, 3, 5, 4, 4, 2, 2, 2, 2, 3, 2, 2, 4, 2, 16, 2, 3, 15, 2, 15, 15, 3, 2, 14, 2, 4, 3, 2, 3, 3, 2, 18, 3, 2, 15, 2, 2, 3, 2, 14, 2, 2, 2, 2, 2, 2, 2, 2, 2, 2, 2, 2, 4, 2, 2, 2, 2, 2, 2, 14, 2, 14, 2, 2, 2, 2, 2, 2, 5, 2, 2, 2, 14, 2, 2, 2, 2, 2, 14, 2, 5, 2, 2, 6, 13, 5, 4, 2, 2, 2, 2, 2, 2, 2, 2, 2, 2, 2, 2, 2, 4, 4, 5, 4, 4, 4, 4, 2	18	979	73.44 s

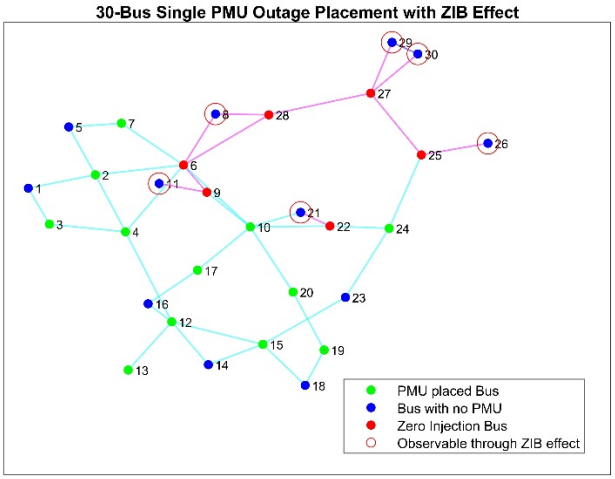

Figure 11. SPO 30-bus placement with ZIB effect indicating nodes with no PMUs placed (blue), PMU placed (green), ZIB nodes (red) and node observed through ZIB effect in a (red cycle), and lines with direct (cyan), pseudo (blue) and virtual (violet) measurements.

Table 7. PMU placement summary of cases 1–4.

	Optimal Number of PMUs			
IEEE Test System	**Case 1**	**Case 2**	**Case 3**	**Case 4**
14-bus	4	3	9	7
30-bus	10	6	21	12
39-bus	13	7	28	16
57-bus	17	12	36	23
118-bus	32	28	68	60
300-bus	91	65	204	143

5.5. Algorithm Efficacy on Large-Sale Power Systems

The effectiveness of the proposed BFA algorithm in large-scale power grids is assessed across all the cases covered. The comparison of BFA performance against existing methods on these large-scale systems is presented in Table 8. This is performed using Polish 2383 and Polish 3120 test cases, and their placement results are in Table 9 and an example plot of Polish 3120-bus in Figure 12. From Table 8, the BFA algorithm has deployed a few PMUs in Polish 2383-bus than all the methods that it is compared with across case 1 and case 2. In case 3 and case 4, although other researchers have developed algorithms testing these conditions, the BFA algorithm remains unopposed as most researchers have not tested their algorithms' efficacies with large-scale buses under those cases. It is also evident that there is a consistency in the trend observed through IEEE test systems across all cases considered. Therefore, all the arguments made regarding trade-offs in PMU installation costs against system reliability in keeping the entire system observable holds.

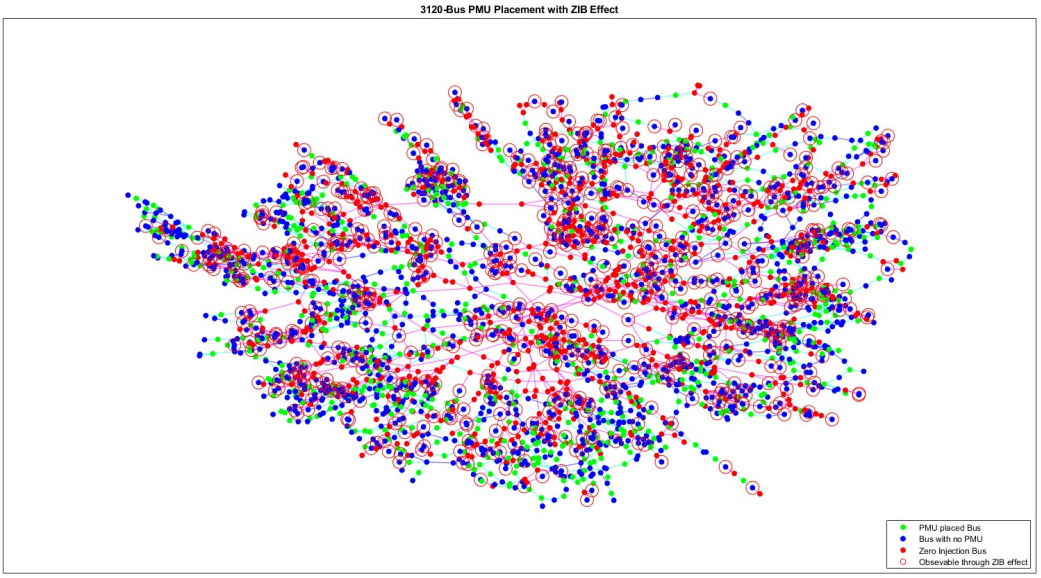

Figure 12. Polish 3120-bus placement with ZIB effect indicating nodes with no PMUs placed (blue), PMU placed (green), ZIB nodes (red) and node observed through ZIB effect in a (red cycle), and lines with direct (cyan), pseudo (blue) and virtual (violet) measurements.

Table 8. Large-scale systems PMU placement comparison with existing methods.

		Case 1		Case 2		Case 3		Case 4	
Method	**Test System**	**Number of PMUs**	**SORI**	**Number of PMUs**	**SORI**	**Number of PMUs**	**SORI**	**Number of PMUs**	**SORI**
Proposed	Polish 2383	829	3325	515	9049	1719	6020	1110	27,138
	Polish 3120	1131	4281	699	19,225	2263	7759	1444	63,216
[44]	Polish 2383	-	-	559	-	-	-	-	-
[28]	Polish 2383	-	-	556	-	-	-	-	-

Table 9. PMU placement of large systems with ZIB effect.

Test System	**PMU Placement**
Polish 2838	105, 125, 187, 192, 207, 213, 217, 218, 223, 226, 229, 230, 233, 235, 237, 239, 240, 245, 246, 247, 249, 255, 257, 259, 265, 267, 273, 277, 278, 279, 282, 285, 287, 288, 295, 299, 300, 314, 315, 316, 319, 320, 324, 325, 326, 334, 339, 347, 350, 353, 360, 365, 366, 368, 370, 377, 378, 380, 384, 385, 388, 392, 393, 394, 404, 408, 409, 411, 424, 425, 431, 432, 434, 437, 438, 442, 443, 444, 445, 446, 448, 456, 459, 462, 464, 468, 472, 475, 476, 481, 486, 488, 493, 494, 497, 502, 505, 508, 510, 511, 512, 514, 515, 523, 525, 527, 529, 530, 533, 535, 544, 547, 548, 550, 553, 563, 567, 579, 583, 584, 589, 591, 593, 594, 595, 601, 602, 603, 605, 618, 621, 624, 636, 637, 643, 646, 648, 649, 650, 653, 661, 666, 668, 671, 676, 678, 679, 680, 685, 690, 691, 694, 695, 703, 704, 710, 718, 720, 721, 723, 724, 728, 733, 742, 745, 747, 749, 750, 752, 755, 756, 758, 762, 763, 765, 768, 774, 775, 776, 778, 781, 785, 794, 796, 798, 802, 834, 835, 839, 849, 852, 858, 859, 860, 862, 870, 871, 877, 883, 891, 892, 895, 899, 908, 910, 913, 914, 920, 943, 949, 954, 957, 961, 964, 968, 973, 978, 979, 995, 996, 997, 998, 1024, 1058, 1059, 1077, 1079, 1082, 1097, 1104, 1107, 1117, 1138, 1140, 1141, 1143, 1149, 1154, 1155, 1168, 1169, 1179, 1183, 1184, 1190, 1191, 1192, 1201, 1206, 1207, 1216, 1217, 1229, 1234, 1240, 1241, 1245, 1250, 1251, 1278, 1284, 1285, 1308, 1326, 1328, 1329, 1330, 1337, 1345, 1346, 1351, 1366, 1374, 1375, 1389, 1393, 1402, 1410, 1415, 1416, 1418, 1421, 1426, 1427, 1430, 1450, 1453, 1454, 1462, 1469, 1475, 1476, 1483, 1486, 1489, 1500, 1505, 1512, 1513, 1514, 1517, 1518, 1528, 1533, 1534, 1536, 1540, 1543, 1546, 1552, 1553, 1556, 1565, 1566, 1576, 1579, 1580, 1584, 1585, 1594, 1598, 1605, 1610, 1616, 1617, 1619, 1620, 1622, 1623, 1625, 1639, 1641, 1642, 1643, 1652, 1656, 1658, 1660, 1661, 1668, 1674, 1675, 1676, 1680, 1683, 1688, 1690, 1691, 1697, 1700, 1702, 1703, 1717, 1728, 1733, 1734, 1739, 1743, 1752, 1755, 1757, 1760, 1761, 1766, 1772, 1784, 1786, 1787, 1793, 1794, 1796, 1801, 1809, 1825, 1826, 1829, 1836, 1837, 1838, 1844, 1845, 1847, 1860, 1867, 1871, 1873, 1882, 1883, 1884, 1886, 1889, 1891, 1894, 1900, 1918, 1921, 1924, 1926, 1934, 1946, 1949, 1950, 1957, 1963, 1970, 1976, 1983, 1985, 1986, 1991, 1993, 1998, 2006, 2007, 2011, 2013, 2018, 2021, 2023, 2032, 2036, 2037, 2042, 2043, 2044, 2045, 2047, 2048, 2052, 2054, 2056, 2058, 2085, 2087, 2088, 2091, 2093, 2095, 2096, 2099, 2100, 2105, 2106, 2119, 2122, 2124, 2127, 2132, 2137, 2140, 2145, 2146, 2151, 2152, 2154, 2155, 2160, 2167, 2168, 2172, 2173, 2175, 2190, 2191, 2195, 2196, 2199, 2202, 2203, 2204, 2209, 2212, 2217, 2218, 2224, 2229, 2231, 2232, 2233, 2235, 2240, 2242, 2244, 2245, 2247, 2251, 2255, 2265, 2267, 2268, 2270, 2271, 2274, 2281, 2283, 2286, 2288, 2293, 2298, 2304, 2305, 2306, 2310, 2311, 2313, 2323, 2324, 2331, 2336, 2339, 2342, 2350, 2372, 2374, 2375
Polish 3120	20, 35, 42, 46, 48, 59, 63, 69, 72, 74, 78, 83, 89, 95, 97, 98, 101, 107, 110, 111, 117, 121, 124, 129, 130, 133, 138, 150, 153, 154, 156, 160, 163, 167, 169, 173, 174, 177, 179, 184, 185, 187, 194, 196, 201, 208, 210, 215, 219, 222, 225, 229, 235, 236, 240, 241, 243, 245, 248, 249, 252, 260, 264, 270, 274, 278, 281, 282, 287, 289, 291, 292, 297, 299, 302, 303, 304, 306, 308, 310, 311, 312, 313, 318, 321, 327, 328, 333, 336, 338, 343, 345, 348, 350, 353, 363, 364, 365, 366, 367, 369, 373, 374, 378, 379, 382, 385, 388, 390, 392, 393, 394, 396, 401, 407, 409, 410, 414, 415, 421, 422, 429, 435, 438, 440, 442, 443, 446, 450, 452, 455, 461, 463, 464, 467, 470, 472, 474, 478, 479, 483, 485, 486, 488, 489, 491, 492, 497, 499, 501, 505, 506, 509, 511, 513, 514, 516, 518, 520, 522, 526, 533, 536, 541, 548, 550, 565, 567, 569, 570, 575, 580, 583, 585, 590, 594, 605, 608, 609, 612, 615, 617, 619, 627, 629, 635, 638, 639, 641, 642, 647, 648, 650, 651, 656, 658, 661, 667, 669, 671, 676, 678, 681, 682, 685, 687, 694, 696, 700, 701, 702, 706, 709, 714, 722, 723, 733, 739, 740, 741, 742, 743, 744, 750, 752, 754, 760, 761, 763, 764, 766, 767, 768, 773, 774, 780, 785, 786, 789, 790, 796, 800, 805, 807, 811, 813, 815, 818, 820, 822, 830, 832, 838, 839, 841, 842, 845, 848, 850, 852, 853, 858, 865, 868, 871, 874, 875, 878, 883, 887, 891, 896, 902, 903, 910, 915, 923, 932, 935, 939, 940, 945, 947, 949, 950, 952, 956, 963, 966, 969, 971, 972, 986, 989, 991, 1010, 1012, 1013, 1020, 1022, 1033, 1034, 1035, 1036, 1040, 1043, 1044, 1048, 1050, 1054, 1055, 1060, 1069, 1073, 1074, 1085, 1090, 1093, 1095, 1096, 1098, 1102, 1105, 1106, 1110, 1116, 1117, 1125, 1126, 1127, 1131, 1134, 1139, 1146, 1149, 1152, 1153, 1154, 1155, 1157, 1158, 1163, 1165, 1166, 1169, 1171, 1180, 1181, 1184, 1187, 1190, 1192, 1194, 1198, 1201, 1202, 1205, 1211, 1213, 1217, 1221, 1225, 1230, 1237, 1239, 1241, 1245, 1246, 1248, 1252, 1253, 1255, 1258, 1260, 1261, 1271, 1273, 1277, 1280, 1285, 1289, 1290, 1291, 1292, 1299, 1302, 1307, 1310, 1311, 1314, 1320, 1322, 1326, 1327, 1331, 1335, 1347, 1348, 1353, 1354, 1356, 1357, 1359, 1360, 1364, 1367, 1370, 1375, 1377, 1378, 1380, 1382, 1383, 1384, 1385, 1386, 1389, 1391, 1414, 1415, 1417, 1419, 1424, 1425, 1426, 1432, 1433, 1434, 1435, 1436, 1442, 1443, 1445, 1447, 1448, 1449, 1452, 1456, 1459, 1464, 1467, 1469, 1470, 1478, 1486, 1490, 1491, 1492, 1500, 1504, 1508, 1510, 1511, 1515, 1518, 1519, 1526, 1527, 1530, 1535, 1539, 1541, 1543, 1545, 1547, 1548, 1550, 1551, 1553, 1555, 1559, 1562, 1569, 1574, 1576, 1579, 1586, 1587, 1588, 1589, 1590, 1592, 1595, 1596, 1609, 1612, 1613, 1614, 1615, 1619, 1621, 1625, 1627, 1628, 1629, 1634, 1639, 1641, 1645, 1648, 1655, 1662, 1664, 1680, 1681, 1685, 1687, 1690, 1692, 1698, 1699, 1708, 1716, 1719, 1730, 1731, 1733, 1736, 1743, 1744, 1752, 1753, 1755, 1760, 1766, 1769, 1770, 1781, 1789, 1790, 1791, 1792, 1793, 1796, 1802, 1803, 1812, 1819, 1824, 1829, 1832, 1833, 1834, 1835, 1836, 1837, 1840, 1845, 1847, 1849, 1856, 1861, 1862, 1863, 1865, 1866, 1867, 1869, 1871, 1877, 1883, 1885, 1886, 1889, 1893, 1898, 1899, 1901, 1907, 1908, 1910, 1911, 1914, 1916, 1925, 1927, 1929, 1930, 1937, 1940, 1942, 1944, 1952, 1953, 1957, 1959, 1961, 1964, 1967, 1969, 1971, 1972, 1976, 1980, 1981, 1988, 1989, 1992, 1993, 1994, 1997, 2000, 2001, 2010, 2011, 2014, 2015, 2016, 2019, 2020, 2021, 2029, 2030, 2038, 2042, 2044, 2046, 2047, 2050, 2053, 2060, 2073, 2074, 2075, 2082, 2083, 2086, 2100, 2101, 2107, 2108, 2109, 2114, 2122, 2123, 2132, 2133, 2134, 2141, 2143, 2147, 2149, 2150, 2152, 2155, 2159, 2161, 2162, 2166, 2168, 2169, 2170, 2174, 2178, 2181, 2184, 2187, 2188, 2195, 2199, 2202, 2204, 2205, 2219, 2223, 2224, 2225, 2226, 2230, 2232, 2233, 2236, 2243, 2244, 2245, 2246, 2249, 2252, 2253, 2255, 2256, 2257, 2259, 2262, 2263, 2265, 2269, 2274, 2277, 2278, 2279, 2286, 2288, 2297, 2299, 2300, 2301, 2302, 2307

5.6. ZIB Effect Propagation Evaluations

The effect of ZIBs is used in the BFA as a strategy to reduce PMU installation costs in cases 2 and 4. The implications of the ZIB effect have also been discussed while considering security concerns with regards to the continuity of current through the ZIIR. Table 10 details different evaluation metrics used to quantify the impact of the ZIB effect utilization. In this study, ZIUR is calculated using buses that are only observable through the ZIB effect divided by $\boldsymbol{Z_T}$. There are buses seen through both the ZIB effect and the direct measurement of PMUs; this is beneficial to the system since there is more than one path leading to the observability of a bus, but those buses are not included in calculating the true utilization rate of ZIBs in the system. The deepest propagation path through the ZIIR is presented in Table 10 in the form of PMU-placed bus/ZIIR/Observed bus and lists all the individual buses contributing to the maximum ZIOD in the system. The maximum ZIOD reveals the level of vulnerability that the system has; the higher it is, the more susceptible the systems are to the loss of observability of many nodes. Should one ZIB drop out due to any form of failure along the ZIIR contributing to the ZIOD, it can render many buses unobservable. In case 2, IEEE 30-bus has the deepest ZIIR propagation path at 10:9, 6, 28, 27, 25:26. The ZIIR in this path is observable through PMUs installed on bus 2, 4 and 10. Any fault between buses 2, 4 or 10 and bus 26—resulting in the loss of power along the ZIIR—will make buses 7, 8, 11, 24, 26, 29, 30 and, in the worst-case scenario, the entire ZIIR unobservable. It becomes clear that the higher the ZIUR rate the system has, the more it becomes susceptible to the loss of system observability due to heavy reliance on ZIBs. In case 4, where BFA solves the OPP satisfying the SPO constraint that guards against single PMU loss in conjunction with employing the ZIB effect, it is confirmed that it is possible to strike a balance between reliability and PMU installation costs. The evidence of this is that ZIUR across all buses reduced from case 2 to case 4. This means that observability through PMUs has increased significantly.

Table 10. ZIB effect propagations observability analysis.

Case	Test Systems	Number of ZIB Buses	Optimal Number of PMUs	Buses Observable through Both Direct PMU Measurement and ZIB Effect	Buses Observable through ZIB Effect Only	Max ZIOD	Deepest Propagation Path through ZIIR	ZIUR (%)
2	14-Bus	1	3	-	8	2	4:7:8	100
	30-Bus	6	6	21	7, 8, 11, 24, 26, 29, 30	6	10:9, 6, 28, 27, 25:26	116.6
	39-Bus	10	7	7, 21, 15	3, 4, 12, 18, 27, 30, 33.35	7	8:4, 6, 11, 10, 13, 14:4	80
	57-Bus	15	12	8, 13, 14, 38, 41, 57	5, 6, 23, 27, 35, 43, 47	5	27:26, 24:23	46.6
4	14-Bus	1	7	-	8	2	4:7:8	100
	30-Bus	6	12	21	8, 11, 26, 29, 30	6	10:9, 6, 28, 27, 25:26	83.3
	39-Bus	10	16	4, 7, 18, 27	12, 30, 31, 32, 33, 35	6	15:14, 13, 10, 11, 6:31	60
	57-Bus	15	23	5, 8, 14, 43, 44, 57	23, 35, 47	3	38:37, 36:35	20

5.7. BFA Computational Time

The time taken by the BFA to solve the OPP for any given system is presented in each case study. Across all the case studies, a general trend is that the larger the system, the longer the BFA will take to solve the OPP problem. In cases where SPO constraint with and without ZIB effect is considered, the permutation is fewer; hence, possible solutions are reduced. Because of this, BFA finds the optimal solution within the first or second iteration. It is also observed that, in cases where the ZIB effect is considered, the algorithm tends to be faster than when it is not considered. This is due to the graph reconstruction procedure used that led to a reduction in nodes in the search space. Even though the IEEE test cases used are inspired by real EPS systems, there is no direct relationship between

the BFA computational time on each of the test systems used. This is because test systems are random power graphs in nature that do not follow clear-cut rules for construction and extensions but rather are a consideration of places where power is needed. This notion of random power graphs is well-explained in [36]. In general, when the BFA computational time is compared with those from other OPP algorithms, its performance varies; in some cases, it performs better than existing methods because the i_{SF} traverses the search space in a strategic manner, similarly to the firefly, in accordance with its bio-objectives in the real world. In some cases, the existing OPP algorithms perform better, as shown in Table 11. There are several factors that influence the BFA performance like the starting node of the search agent, which may influence the trajectory of the search. This is because the BFA can start the search from any random node. The computational environment also plays a significant role on determining how fast the optimization is carried out. The authors of [44] report having used IBM CPLEX, which has proven to increase the computational ability of the system used, especially with large-scale systems. Table 11 also shows that in terms of computational time, the BFA takes longer than the existing algorithm in [44]. This limitation is due to, amongst other reasons, the time taken to construct the undirected graphs before the search agent transverses the search space. Even though the proposed BFA has a limitation of taking longer than ILP-based methods to solve the OPP problem, the algorithm can still be used for less time-sensitive applications like power network planning and extensions, as highlighted in [27].

Table 11. Computational time comparison with existing methods.

Case 1: Normal Operation without ZIB Effect and Unlimited Channel Limits								
Refs.	14-Bus	30-Bus	39-Bus	57-Bus	118-Bus	300-Bus	Polish 2383-Bus	Polish 3120-Bus
Proposed	0.847 s	0.761 s	1.418 s	3.892 s	2896.1 s	1015 s	3625.7 s	7989.3 s
[27]	1.11 s	3.53 s	-	24.87 s	-	-	-	-
[45]	1.855 s	7.886 s	-	16.425 s	38.347 s	-	-	-
[32]	0.008 s	0.013 s	0.014 s	0.071 s	0.036 s	0.189 s	-	-
Case 2: Normal Operation with ZIB Effect Consideration								
Refs.	14-Bus	30-Bus	39-Bus	57-Bus	118-Bus	300-Bus	Polish 2383-Bus	Polish 3120-Bus
Proposed	2.58	3.04	2.64	2.73	440.5		3252.9 s	6298.1 s
[27]	1.2	3.0	-	53.4	-	-	-	-
[44]	0.1101	0.1547	0.2084	-	0.1984	-	2.5888	-
[45]	1.664 s	4.572 s	-	11.243 s	34.136 s			
Case 3: Single PMU Outage								
Refs.	14-Bus	30-Bus	39-Bus	57-Bus	118-Bus	300-Bus	Polish 2383-Bus	Polish 3120-Bus
Proposed	0.79	0.73	0.83	1.1	3.72	69.3	4116.5 s	5331.1 s
[27]	1.9	4156.1	-	37,050.2	-	-	-	-
[46]	2.357 s	3.450 s	-	7.216 s	-	-	-	-
[47]	-	-	-	-	-	-	0.062 s	-
Case 4: Single PMU Outage with ZIB Effect								
Refs.	14-Bus	30-Bus	39-Bus	57-Bus	118-Bus	300-Bus	Polish 2383-Bus	Polish 3120-Bus
Proposed	1.38 s	1.63 s	1.74 s	2.0 s	4.44 s	73.44 s	3003.2 s	4528 s
[27]	1.4 s	153.3 s	-	37,050.2 s	-	-	-	-
[44]	0.1 s	0.2 s	0.2 s	-	0.2 s	-	3.1 s	-
[47]	0.014 s	0.098 s	0.247 s	-	0.862 s	-	4889 s	-

5.8. BFA Sensitivity Analysis

This section presents an experimental analysis of the BFA algorithm to establish the most effective parameter settings. In this study, it is important to recognise two of the most common parameters among meta-heuristic algorithms: these are population size and the maximum number of algorithm iterations. It is crucial to maintain that in this approach, there is no flexibility in population size since it was dictated by the number of nodes from a given IEEE test system, and that for all the cases, iterations were kept at the maximum of 200. In the BFA algorithm, in Equation (9), one can realize that the attractiveness of the i_{SF} depends on the exponential term, which carries light absorption (γ). To establish the sensitivity of the BFA algorithm, the light absorption of the i_{SF} was varied in steps of 0.2 within the range $\gamma \in [0-1]$ and the execution time to reach the optimal number of PMUs was noted. Based on the convergence histories of different IEEE bus systems used, the lower the light absorption value, the longer it takes for the system to find to converge to the optimal number, as shown by Figure 13, which represents the convergence histories of Case 4 in terms of computational time.

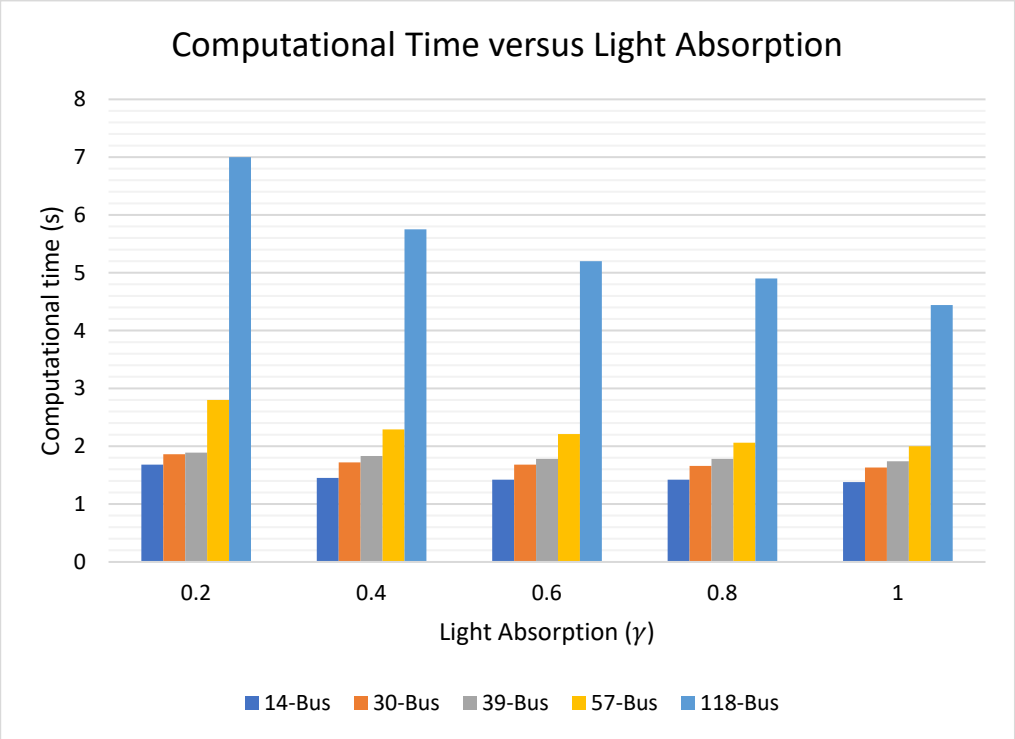

Figure 13. BFA computational times for different values of light absorption values.

5.9. BFA Comparison with Existing OPP Algorithms

In this section, BFA results are compared with the most recent existing methods in the same test systems under the same case studies. In Tables 12 and 13, the basis of comparison is on the optimal number of PMU each method achieved as well as the SORI for each PMU placement solution set. The presentation is such that each system has the number of PMUs, followed by the SORI value in brackets. For normal operations, Case 1, the proposed algorithm, has achieved the same number of PMUs but better if not the same SORI values across all the test EPS systems than its counterparts. In case 2, the proposed algorithm still has the same number of PMUs or less than other methods, for example, in 30-Bus, BFA registered six PMUs, similarly as in [32], but a SORI value of 51, which is the highest in that column. Nevertheless, under case 2, BFA also registered the lowest PMU number of 7 for bus 39 with a SORI of 40. For cases 3 and 4, Table 13 is almost empty; this shows that a large amount of work still needs to be conducted as these cases are the highlights for an improved reliability of measurement with the reduction in PMU installation cost in

mind. In case 3, BFA found the same or lower number of PMUs and higher SORI values, except with the IEEE 57-bus. The same is for case 4, whereby BFA recorded the lowest PMU numbers except under IEEE 57-bus, where [30] recorded 22 PMUs against 23 obtained by BFA.

Table 12. Comparison of BFA with existing methods under Case 1 and Case 2.

Year	Refs.	Optimal Number of PMUs											
		Case 1						Case 2					
		14-Bus	30-Bus	39-Bus	57-Bus	118-Bus	300-Bus	14-Bus	30-Bus	39-bus	57-Bus	118-Bus	300-Bus
N/A	Proposed	14-Bus	30-Bus	39-bus	57-Bus	118-Bus	300-Bus	14-Bus	30-Bus	39-bus	57-Bus	118-Bus	300-Bus
2022	[27]	4 (19)	10 (52)	13 (52)	17 (72)	32 (164)	96 (419)	3 (15)	6 (51)	7 (40)	12 (59)	28 (174)	65 (528)
2020	[28]	4 (16)	10 (48)	-	17 (69)	-	-	3	7	-	12	-	-
2020	[48]	-	-	13	17	32	-	-	-	8	11	28	-
2020	[30]	4 (17)	10 (51)	13 (52)	17 (71)	32 (157)	-	3 (15)	7 (29)	8 (32)	12 (49)	29 (143)	-
2019	[32]	4	10	13	17	32	-	3	6	8	11	28	-
2018	[44]	4 (19)	10 (52)	13 (52)	-	32 (163)	-	3 (16)	6 (37)	8 (45)	-	28 (156)	-
2018	[33]	4	10	13	-	32	-	3	7	8	-	28	-
2018	[33]	-	-	-	-	-	-	3	7	9	12	29	-
2015	[49]	-	-	-	-	-	-	3	7	9	12	29	74

Table 13. Comparison of BFA with existing methods under Case 3 and Case 4.

Year	Refs.	Optimal Number of PMUs											
		Case 3						Case 4					
		14-Bus	30-Bus	39-bus	57-Bus	118-Bus	300-Bus	14-Bus	30-Bus	39-bus	57-Bus	118-Bus	300-Bus
N/A	Proposed	9 (39)	21 (85)	28 (96)	36 (148)	68 (323)	204 (788)	7 (33)	12 (85)	16 (74)	23 (115)	60 (339)	143 (979)
2022	[27]	9	21	-	25	-	-	7	15	-	25	-	--
2020	[28]	-	-	-	-	-	-	-	-	-	-	-	-
2020	[48]	9 (39)	21 (83)	29 (99)	33 (129)	69 (313)	-	-	-	-	-	-	-
2020	[30]	-	-	-	-	-	-	7	14	17	22	61	-
2019	[32]	-	-	-	-	-	-	-	-	-	-	-	-
2018	[44]	-	-	-	-	-	-	7	14	19	-	64	-
2018	[33]	-	-	-	-	-	-	7	16	19	27	62	-
2018	[33]	-	-	-	-	-	-	-	-	-	-	-	-
2015	[49]	-	-	-	-	-	-	-	-	-	-	-	-

6. Conclusions

The results obtained by using BFA on IEEE test systems across all case studies confirm that it can solve the OPP problem without becoming stuck to the local minima. BFA can find multiple PMU placement sets of the same optimal PMU number similarly to other meta-heuristic algorithms. BFA solved the OPP problem by avoiding PMU placement on radial bus locations based on their low node C_D scores as considered in a ranked undirected power network graph. BFA achieved the same results obtained by the existing methods which it is compared to, but takes an upper hand as shown by BOI and TSORI scores. PMU placement under normal conditions without the consideration of the ZIB effect results in an unreliable and high cost of PMU installation. The utilization of the ZIB effect under normal operation reduced PUM installation costs but significantly elevated the chances of unobservability of any system should there be a fault affecting the availability of measurements. SPO was investigated using BFA by satisfying the observability constraint that ensured each bus would be observed directly at least by two PMUs. BFA algorithm, when considering SPO without the ZIB effect, is robust against faults but nearly doubles the cost of Case 1. To reduce these PMU installation costs, BFA considered SPO with ZIB effect, resulting in a reduced ZIUR, which is good for system observability. Furthermore, these results

with large-scale simulation systems and the algorithm's results are consistent throughout. The BFA computational times show that it has several limitations when compared with some of the existing algorithms. This is due to a randomized start that may affect the path taken by the search agent. This can be improved by using machine learning in graphical approach, where several node-level features—instead of only the degree centrality and graph structure-based features—can be used to train the PMU placement model that will be applicable to a variety of power system network sizes.

Author Contributions: Conceptualization, O.T.; Methodology, O.T., M.M. and T.S.; Software, O.T. and T.S.; Validation, R.S., B.M. and M.M.; Writing—original draft, O.T.; Writing—review & editing, B.M.; Supervision, R.S., B.M. and M.M. All authors have read and agreed to the published version of the manuscript.

Funding: This research received no external funding.

Data Availability Statement: Publicly available datasets were analysed in this study. This data can be found here: https://matpower.org/docs/ref/matpower5.0/menu5.0.html (accessed on 2 August 2023).

Acknowledgments: I would like to thank all the co-authors of this paper for all their valuable efforts and advice in this research.

Conflicts of Interest: The authors declare no conflict of interest.

References

1. Gamboa, S.; Orduña, E. Hierarchically Distributed Architecture for Large-Scale Integrated WAMPAC System. In Proceedings of the 2015 International Conference on Electronics, Communications and Computers (CONIELECOMP), Cholula, Mexico, 25–27 February 2015; pp. 16–20.
2. Guo, X.-C.; Liao, C.-S.; Chu, C.-C. Decentralized PMU Placements in a Dynamic Programming Approach. In Proceedings of the 2019 IEEE Industry Applications Society Annual Meeting, Baltimore, MD, USA, 29 September–3 October 2019; pp. 1–8.
3. Blair, S.M.; Syed, M.H.; Roscoe, A.J.; Burt, G.M.; Braun, J. Measurement and Analysis of PMU Reporting Latency for Smart Grid Protection and Control Applications. *IEEE Access* **2019**, *7*, 48689–48698. [CrossRef]
4. *IEEE Std C37.118.1a-2014 (Amendment to IEEE Std C37.118.1-2011)*; IEEE Standard for Synchrophasor Measurements for Power Systems—Amendment 1: Modification of Selected Performance Requirements. IEEE Standards Association: Piscataway, NJ, USA, 2014; pp. 1–25. [CrossRef]
5. Specialized Protection/Control. Available online: https://www.gegridsolutions.com/multilin/catalog/p847.htm (accessed on 21 October 2022).
6. Maji, T.K.; Acharjee, P. Multiple Solutions of Optimal PMU Placement Using Exponential Binary PSO Algorithm for Smart Grid Applications. *IEEE Trans. Ind. Appl.* **2017**, *53*, 2550–2559. [CrossRef]
7. Xu, J.; Wen, M.H.F.; Li, V.O.K.; Leung, K.-C. Optimal PMU Placement for Wide-Area Monitoring Using Chemical Reaction Optimization. In Proceedings of the 2013 IEEE PES Innovative Smart Grid Technologies Conference (ISGT), Washington, DC, USA, 24–27 February 2013; pp. 1–6.
8. Bombieri, N.; Pravadelli, G.; Fujita, M.; Austin, T.; Reis, R. *VLSI-SoC: Design and Engineering of Electronics Systems Based on New Computing Paradigms: 26th IFIP WG 10.5/IEEE International Conference on Very Large Scale Integration, VLSI-SoC 2018, Verona, Italy, 8–10 October 2018, Revised and Extended Selected Papers*; Springer: Berlin/Heidelberg, Germany, 2019; ISBN 978-3-030-23425-6.
9. Shalini; Samantaray, S.R.; Sharma, A. Enhancing Performance of Wide-Area Back-Up Protection Scheme Using PMU Assisted Dynamic State Estimator. *IEEE Trans. Smart Grid* **2019**, *10*, 5066–5074. [CrossRef]
10. Johnson, T.; Moger, T. A Critical Review of Methods for Optimal Placement of Phasor Measurement Units. *Int. Trans. Electr. Energy Syst.* **2021**, *31*, e12698. [CrossRef]
11. Ahmed, M.M.; Amjad, M.; Qureshi, M.A.; Imran, K.; Haider, Z.M.; Khan, M.O. A Critical Review of State-of-the-Art Optimal PMU Placement Techniques. *Energies* **2022**, *15*, 2125. [CrossRef]
12. Gharani Khajeh, K.; Bashar, E.; Mahboub Rad, A.; Gharehpetian, G.B. Integrated Model Considering Effects of Zero Injection Buses and Conventional Measurements on Optimal PMU Placement. *IEEE Trans. Smart Grid* **2017**, *8*, 1006–1013. [CrossRef]
13. Nagananda, K.G.; Kishore, S.; Blum, R.S. A PMU Scheduling Scheme for Transmission of Synchrophasor Data in Electric Power Systems. *IEEE Trans. Smart Grid* **2015**, *6*, 2519–2528. [CrossRef]
14. Manousakis, N.M.; Korres, G.N. A Weighted Least Squares Algorithm for Optimal PMU Placement. *IEEE Trans. Power Syst.* **2013**, *28*, 3499–3500. [CrossRef]
15. Joshi, P.M.; Verma, H.K. Synchrophasor Measurement Applications and Optimal PMU Placement: A Review. *Electr. Power Syst. Res.* **2021**, *199*, 107428. [CrossRef]
16. Aminifar, F.; Lucas, C.; Khodaei, A.; Fotuhi-Firuzabad, M. Optimal Placement of Phasor Measurement Units Using Immunity Genetic Algorithm. *IEEE Trans. Power Deliv.* **2009**, *24*, 1014–1020. [CrossRef]

17. Milosevic, B.; Begovic, M. Nondominated Sorting Genetic Algorithm for Optimal Phasor Measurement Placement. *IEEE Trans. Power Syst.* **2003**, *18*, 69–75. [CrossRef]
18. Andreoni, R.; Macii, D.; Brunelli, M.; Petri, D. Tri-Objective Optimal PMU Placement Including Accurate State Estimation: The Case of Distribution Systems. *IEEE Access* **2021**, *9*, 62102–62117. [CrossRef]
19. Theodorakatos, N.P. Optimal Phasor Measurement Unit Placement for Numerical Observability Using Branch-and-Bound and a Binary-Coded Genetic Algorithm. *Electr. Power Compon. Syst.* **2019**, *47*, 357–371. [CrossRef]
20. Li, W.; Deka, D.; Chertkov, M.; Wang, M. Real-Time Faulted Line Localization and PMU Placement in Power Systems through Convolutional Neural Networks. *IEEE Trans. Power Syst.* **2019**, *34*, 4640–4651. [CrossRef]
21. Rezaeian Koochi, M.H.; Dehghanian, P.; Esmaeili, S. PMU Placement with Channel Limitation for Faulty Line Detection in Transmission Systems. *IEEE Trans. Power Deliv.* **2020**, *35*, 819–827. [CrossRef]
22. Shi, Y.; Tuan, H.D.; Duong, T.Q.; Poor, H.V.; Savkin, A.V. PMU Placement Optimization for Efficient State Estimation in Smart Grid. *IEEE J. Sel. Areas Commun.* **2020**, *38*, 71–83. [CrossRef]
23. Bonavolontà, F.; Noia, L.P.D.; Liccardo, A.; Tessitore, S.; Lauria, D. A PSO-MMA Method for the Parameters Estimation of Interarea Oscillations in Electrical Grids. *IEEE Trans. Instrum. Meas.* **2020**, *69*, 8853–8865. [CrossRef]
24. Rahman, N.H.A.; Zobaa, A.F. Integrated Mutation Strategy with Modified Binary PSO Algorithm for Optimal PMUs Placement. *IEEE Trans. Ind. Inform.* **2017**, *13*, 3124–3133. [CrossRef]
25. Appasani, B.; Mohanta, D.K. Co-Optimal Placement of PMUs and Their Communication Infrastructure for Minimization of Propagation Delay in the WAMS. *IEEE Trans. Ind. Inform.* **2018**, *14*, 2120–2132. [CrossRef]
26. Arpanahi, M.K.; Alhelou, H.H.; Siano, P. A Novel Multiobjective OPP for Power System Small Signal Stability Assessment Considering WAMS Uncertainties. *IEEE Trans. Ind. Inform.* **2020**, *16*, 3039–3050. [CrossRef]
27. Johnson, T.; Moger, T. Security-Constrained Optimal Placement of PMUs Using Crow Search Algorithm. *Appl. Soft Comput.* **2022**, *128*, 109472. [CrossRef]
28. Guo, X.-C.; Liao, C.-S.; Chu, C.-C. Enhanced Optimal PMU Placements with Limited Observability Propagations. *IEEE Access* **2020**, *8*, 22515–22524. [CrossRef]
29. Rezaeian Koochi, M.H.; Hemmatpour, M.H. A General PMU Placement Approach Considering Both Topology and System Aspects of Contingencies. *Int. J. Electr. Power Energy Syst.* **2020**, *118*, 105774. [CrossRef]
30. Chen, X.; Wei, F.; Cao, S.; Soh, C.B.; Tseng, K.J. PMU Placement for Measurement Redundancy Distribution Considering Zero Injection Bus and Contingencies. *IEEE Syst. J.* **2020**, *14*, 5396–5406. [CrossRef]
31. Shafiullah, M.; Hossain, M.I.; Abido, M.A.; Abdel-Fattah, T.; Mantawy, A.H. A Modified Optimal PMU Placement Problem Formulation Considering Channel Limits under Various Contingencies. *Measurement* **2019**, *135*, 875–885. [CrossRef]
32. Babu, R.; Bhattacharyya, B. Strategic Placements of PMUs for Power Network Observability Considering Redundancy Measurement. *Measurement* **2019**, *134*, 606–623. [CrossRef]
33. Lu, C.; Wang, Z.; Ma, M.; Shen, R.; Yu, Y. An Optimal PMU Placement with Reliable Zero Injection Observation. *IEEE Access* **2018**, *6*, 54417–54426. [CrossRef]
34. Koutsoukis, N.C.; Manousakis, N.M.; Georgilakis, P.S.; Korres, G.N. Numerical Observability Method for Optimal Phasor Measurement Units Placement Using Recursive Tabu Search Method. *IET Gener. Transm. Distrib.* **2013**, *7*, 347. [CrossRef]
35. Wang, B.; Liu, D.; Li, X. An Improved Ant Colony System in Optimizing Power System PMU Placement Problem. In Proceedings of the 2009 Asia-Pacific Power and Energy Engineering Conference, Wuhan, China, 27–31 March 2009; pp. 1–3.
36. Shahraeini, M.; Alvandi, A.; Khormali, S. Behavior Analysis of Random Power Graphs for Optimal PMU Placement in Smart Grids. In Proceedings of the 2020 10th International Conference on Computer and Knowledge Engineering (ICCKE), Mashhad, Iran, 29–30 October 2020; pp. 107–112.
37. Rios, M.A.; Gómez, O. Identification of Coherent Groups and PMU Placement for Inter-Area Monitoring Based on Graph Theory. In Proceedings of the 2011 IEEE PES Conference on Innovative Smart Grid Technologies Latin America (ISGT LA), Medellin, Colombia, 19–21 October 2011; pp. 1–7.
38. von Meier, A.; Stewart, E.; McEachern, A.; Andersen, M.; Mehrmanesh, L. Precision Micro-Synchrophasors for Distribution Systems: A Summary of Applications. *IEEE Trans. Smart Grid* **2017**, *8*, 2926–2936. [CrossRef]
39. Li, J.; Wei, X.; Li, B.; Zeng, Z. A Survey on Firefly Algorithms. *Neurocomputing* **2022**, *500*, 662–678. [CrossRef]
40. Nuqui, R.F.; Phadke, A.G. Phasor Measurement Unit Placement Techniques for Complete and Incomplete Observability. *IEEE Trans. Power Deliv.* **2005**, *20*, 2381–2388. [CrossRef]
41. Guo, X.-C.; Liao, C.-S.; Chu, C.-C. Optimal PMU Placements under Propagation Depth Constraints by Mixed Integer Linear Programming. In Proceedings of the 2016 IEEE International Conference on Smart Grid Communications (SmartGridComm), Sydney, NSW, Australia, 6–9 November 2016; pp. 656–661.
42. Awon, M.; Butt, H.Z.; Abdullah Khalid, H.; Janjua, A.K. System Redundancy Index Based Optimized Phasor Measurement Unit Placement for Complete Network Observability. In Proceedings of the 2018 International Conference on Power Generation Systems and Renewable Energy Technologies (PGSRET), Islamabad, Pakistan, 10–12 September 2018; pp. 1–5.
43. Sushma, G.C.; Jyothsna, T.R. Observability Constrained GA Approach for Optimal PMU Placement Considering Zero Injection Modeling. In Proceedings of the 2018 International Conference on Control, Power, Communication and Computing Technologies (ICCPCCT), Kannur, India, 23–24 March 2018; pp. 174–178.

44. Abdulrahman, I.; Radman, G. ILP-Based Optimal PMU Placement with the Inclusion of the Effect of a Group of Zero-Injection Buses | SpringerLink. Available online: https://link.springer.com/article/10.1007/s40313-018-0389-4 (accessed on 22 August 2022).
45. Yuvaraju, V.; Thangavel, S. Optimal Phasor Measurement Unit Placement for Power System Observability Using Teaching–Learning Based Optimization. *Int. J. Electr. Power Energy Syst.* **2022**, *137*, 107775. [CrossRef]
46. Kiio, M.N.; Wekesa, C.W.; Kamau, S.I. Evaluating Performance of a Linear Hybrid State Estimator Utilizing Measurements from RTUs and Optimally Placed PMUs. *IEEE Access* **2022**, *10*, 63113–63131. [CrossRef]
47. Huang, L.; Sun, Y.; Xu, J.; Gao, W.; Zhang, J.; Wu, Z. Optimal PMU Placement Considering Controlled Islanding of Power System. *IEEE Trans. Power Syst.* **2014**, *29*, 742–755. [CrossRef]
48. Abdelsalam, A.A.; Hassanin, K.M.; Abdelaziz, A.Y.; Alhelou, H.H.; Abdelsalam, A.A.; Hassanin, K.M.; Abdelaziz, A.Y.; Alhelou, H.H. Optimal PMUs Placement Considering ZIBs and Single Line and PMUs Outages. *AIMSE* **2020**, *8*, 122–141. [CrossRef]
49. Xia, N.; Gooi, H.B.; Chen, S.X.; Wang, M.Q. Redundancy Based PMU Placement in State Estimation. *Sustain. Energy Grids Netw.* **2015**, *2*, 23–31. [CrossRef]